Quaternary Science Reviews 230 (2020) 106170

Contents lists available at ScienceDirect

Quaternary Science Reviews

journal homepage: www.elsevier.com/locate/quascirev

Abrupt vegetation and environmental change since the MIS 2: A unique paleorecord from Slovakia (Central Europe)

Anna Šolcová [a, b, *], Eva Jamrichová [b, c], Michal Horsák [c], Petr Pařil [c], Libor Petr [c], Oliver Heiri [d], Jiří Květoň [e, f], Marek Křížek [g], Filip Hartvich [g, h], Michal Hájek [c], Petra Hájková [b, c]

[a] Department of Botany, Charles University, Benátská 2, 128 01, Prague, Czech Republic
[b] Laboratory of Paleoecology, Institute of Botany of the Czech Academy of Sciences, Lidická 25/27, 602 00, Brno, Czech Republic
[c] Department of Botany and Zoology, Masaryk University, Kotlářská 2, 611 37, Brno, Czech Republic
[d] Department of Environmental Sciences, University of Basel, Klingelbergstrasse 17, 4056, Basel, Switzerland
[e] Department of Experimental Plant Biology, University of South Bohemia, Branišovská 1716, 370 05, České Budějovice, Czech Republic
[f] Institute of Experimental Botany of the Czech Academy of Sciences, Rozvojová 263, 165 02, Prague, Czech Republic
[g] Department of Physical Geography and Geoecology, Charles University, Albertov 6, 128 43, Prague, Czech Republic
[h] Institute of Rock Structure and Mechanics of the Czech Academy of Sciences, V Holešovičkách 41, 182 09, Prague, Czech Republic

ARTICLE INFO

Article history:
Received 27 November 2019
Received in revised form
12 January 2020
Accepted 12 January 2020
Available online xxx

Keywords:
MIS 2/MIS 1 transition
Lateglacial
Holocene
Paleolimnology
Paleoclimatology
Central Europe
Travertine
Stable isotopes
Chironomids
Vegetation dynamics

ABSTRACT

Research on past abrupt climate change and linked biotic response is essential for understanding of the future development of biota under changing climatic conditions, which, in turn, is necessary for adequate progress in ecosystem management and nature conservation. The present study presents the first comprehensive reconstruction of local and regional environment at the Western Carpathian/Pannonian Basin border, including a first chironomid-based paleoclimate reconstruction and $\delta^{18}O$ and $\delta^{13}C$ records from travertine, to investigate abrupt biota and climate shifts since the Marine Isotope Stage (MIS) 2. A range of biotic and abiotic proxy data in organic-calcareous sediment sequence were analysed using a multi-proxy approach to produce a detailed reconstruction of past ecosystem conditions. The results illustrate that the most prominent abrupt change in the local environment occurred directly at the MIS 2/MIS 1 transition at 14,560 cal BP as a consequence of increased precipitation and an increase in reconstructed mean July temperature by ~2.2 °C. Abrupt changes in local environment during the early Holocene were closely linked to travertine precipitation rate around thermal springs and thus indirectly to the climate until the arrival of the Late Neolithics around 6400 cal BP. Regional vegetation response (derived from pollen data) to the climatic fluctuations lagged, with the most prominent changes around 14,410 cal BP and 10,140 cal BP. Our data suggest the presence of a steppe-tundra ecosystem with evidence for low amounts of temperate broadleaf trees during the MIS 2, indicating close proximity to their northern glacial refugium. We demonstrate the ability of $\delta^{18}O$ and $\delta^{13}C$ stable isotope record from travertine to reflect abrupt climatic and environmental changes. The study provides evidence about benefits using travertine deposits coupled with high-resolution paleoecological data to investigate past biotic and abiotic responses to abrupt climate change.

1. Introduction

Biotic and particularly vegetation responses to past climate change is a frequently studied paleoecological research topic, ranging from investigating the magnitude, speed and direction of ecosystem change, to the resilience and resistance of various ecosystem components to changing climatic conditions (e.g. Feurdean et al., 2014; Randsalu-Wendrup et al., 2012; Camill and Clark, 2000). Information on these aspects of ecosystem change is crucial for modelling future responses to climate development and related nature conservation strategies (Willis and Birks, 2006). In the Quaternary, major vegetation change took place particularly at

* Corresponding author. Department of Botany, Charles University, Benátská 2, 128 01, Praha 2, Czech Republic.
E-mail address: Anna.Potuckova@ibot.cas.cz (A. Šolcová).

https://doi.org/10.1016/j.quascirev.2020.106170
0277-3791/

the interglacial/glacial transitions, where complete replacement of species communities often took place as a consequence of abrupt climate shifts. Pronounced shorter term climatic changes also occurred within interglacial and glacial periods. During the Last Glacial period (114,000–11,700 cal BP), ca 25 abrupt climatic fluctuations known as Dansgaard-Oeschger events occurred (Dansgaard et al., 1993; Rasmussen et al., 2014), during which atmospheric and ocean conditions alternated between relatively mild (interstadial) and cold (stadial) conditions. Unfortunately, continental biotic paleoecological records (e.g. fossil pollen, plant macrofossils) dated back to the Last Glacial or previous Interglacial are only found in exceptional circumstances (e.g. Le Grande Pile, De Beaulieu and Reille, 1992), making it difficult to know how abrupt climatic events impacted terrestrial and aquatic ecosystems.

In the Panonnian Basin (Central-Eastern Europe), loess accumulations are often studied to understand past glacial conditions (Feurdean et al., 2014; Hošek et al., 2017; Sümegi et al., 2012), however, loess accumulations are typically characterised by low pollen and macrofossil preservation making them less than ideal environments to study terrestrial and aquatic ecosystems. Wet environments (lakes, bogs, fens, etc.), which are more suitable for plant fossil preservation and thus more appropriate for environment and vegetation reconstructions, were rare during the MIS 2 (29,000–14,600 cal BP) in the Pannonian Basin (but see e.g. Magyari et al., 1999; Sümegi et al., 2011, 2013) because of cold and dry conditions. In the Pannonian Basin, late Quaternary biotic paleorecords typically span the past 14,600 years (MIS 1) (e.g. Hájková et al., 2013, 2015; Jamrichová et al., 2014; Magyari et al., 2001, 2008; 2010; Petr et al., 2013; Šolcová et al., 2018), which unfortunately do not provide information regarding terrestrial and aquatic ecosystem responses during the MIS 2/MIS 1 transition. Moreover, in the north-western part of the Pannonian Basin, on the Western Carpathian/Pannonian Basin border, older biotic records from MIS 2 are completely missing. It has been suggested that the border between the Western Carpathians and Pannonian Basin provided northern local glacial refugia for temperate biota, as well as provided a relevant migration route (Juřičková et al., 2014, 2018; Sümegi and Náfrádi, 2015; Willis et al., 1995). Detailed studies of past ecosystem change from this region are therefore crucial for better constraining the timing and extent of temperate biota migration after the Last Glacial.

Several paleoclimatological reconstructions from chironomids (Hájková et al., 2016) and calcareous tufa (Juřičková et al., 2018; Dabkowski et al., 2019) have been published from the Western Carpathian/Pannonian Basin border, however, these sites are from mid-to-high elevations (>400 m asl). Currently, no detailed paleoclimatological reconstruction from fossil records exist from lowland sites (below 400 m asl), where precipitation and temperatures would be different in comparison with the mountainous part of the Western Carpathians. Precipitation and the overall water availability for plants were probably the most important environmental drivers determining the distribution of glacial temperate-tree refugia (Willis et al., 2000), as well as determining whether sparse steppe-tundra or hemiboreal (taiga) forests prevailed during MIS 2 in this region. Although the influence of climate on geothermal-related carbonate precipitation (travertine) is considered to be generally less obvious compared with karstic-related carbonate precipitation (calcareous tufa) due to the more complex system of deep hydrothermal water circulation (Capezzuoli et al., 2014), they still provide potential for multidisciplinary studies of past climate changes, associated vegetation development and the evolution of human societies (Šolcová et al., 2018, Prado-Pérez et al., 2013). In the Danubian Lowland (NW part of the Pannonian Basin), numerous thermal springs occur, with a high density near Santovka village (Fig. 1). The first paleoecological investigation of travertine deposits in this region was recently reported (Santovka-village profile; see Šolcová et al., 2018), however this study was chronologically limited to the Holocene. We therefore decided to focus on a second location, Santovka-Pramene Budzgov, situated only ~2 km away from the Santovka-village profile, to provide the first paleoclimatological and paleoecological record dating back to the MIS 2. We applied a multiproxy approach using terrestrial and aquatic proxies (geochemistry, magnetic susceptibility, loss on ignition, pollen, plant macrofossils, chironomids and molluscs) to reconstruct ecosystem function and change over time. Since chironomid assemblages react sensitively to temperature change (Eggermont and Heiri, 2012) chironomid analysis also provides insights on past temperature development at the study site. Stable carbon and oxygen isotopes from travertine carbonates were used to reconstruct whether the basin was influenced by deep or shallow circulation waters, and to constrain the source of CO_2 and detect past climatic fluctuations. In addition, we conducted an electrical resistivity tomography survey to document sub-surface material to better understand the extent of the sedimentation basin. The research objectives of this study are to; 1) reconstruct the regional and local vegetation history during MIS 2; 2) reconstruct temperature variability during the MIS 2/MIS 1 transition at 14,560 cal BP, and investigate the subsequent vegetation response; 3) reveal major abrupt vegetation and environmental changes during the Holocene and determine their causes; and 4) reconstruct deep or shallow circulation waters of calcareous springs and assess the possibility of developing paleoclimate reconstructions from travertine carbonates.

2. Study area

Santovka-Pramene Budzgov (Santovka-PB) is located between the villages of Santovka and Bory near the stream Búr (48°10′12.3″N, 18°45′23.1″E; 150 m asl) (Fig. 1). The study area is formed by andesitic sandstones, overlaid by loess deposits, various deluvial covers and alluvial deposits in the bottom of the valley. The epiclastic andesitic sandstones contain re-deposited tuffs and other fine-grained insets, which are flyschoid in character with interbeddings of pellitic sediment (Nagy et al., 1998). Locally, calcium carbonate-rich springs form travertine mounds (Fig. 3). These springs extract calcium carbonate from the bedrock that is also built by Upper Triassic limestones. The local climate is characterised as warm (8–9 °C mean annual temperature) and dry (550–600 mm mean annual precipitation) (http://geo.enviroportal.sk/atlassr/).

The first permanent human settlement near Santovka village is dated to the Middle Neolithic period (Želiezovce group; 7,000–6,700 cal BP) (Janek, 1972). Human occupation continued during the Late Neolithic (Lengyel I-II culture; ~6,700–6,000 cal BP), with evidence of a large settled area (~25 ha) situated between Santovka and Domadice villages (Budinský-Krička, 1941; Ambros, 1977; Jakab, 1977; Pavúk, 1977, 1987; 1994, 1997; Bača, 1990).

3. Material and methods

3.1. Coring of the paleoecological profile

In May 2015, a 620 cm long profile (333–950 cm from the surface) was obtained from Santovka-PB using a percussion drilling set. The upper 333 cm (0–333 cm) contained clayey flushes from adjacent slopes which were not analysed. During profile coring, it was necessary to break through a consolidated travertine layer present between ~643 and 591 cm, which resulted in missing sediments at these depths. Once obtained, sediment cores were then stored in plastic tubes in the fridge and then sampled at the Department of Botany and Zoology, Masaryk University in Brno.

Fig. 1. Location of the Santovka-Pramene Budzgov study site located in southwest Slovakia (Central-Eastern Europe) on the Western Carpathian/Pannonian Basin border. Locations of other study sites discussed in the text are indicated.

3.2. Electrical resistivity tomography survey

In April 2015, Electrical Resistivity Tomography (ERT) survey was performed at Santovka-PB. ERT is a geophysical subsurface-imaging technique, widely applied in various geoscience studies. Interpretations of results were based on knowledge of the local geology (Nagy et al., 1998), supported by documented profile sedimentary records, and knowledge of geological and geomorphological formations in the area. Altogether, 6 profiles (Figs. 3 and 4) were measured in the area of the infilled paleolake. All ERT profiles used a Wenner-Schlumberger array, which is suitable for expected subhorizontal layering (e.g. Loke, 1997; Engel et al., 2017; Hošek et al., 2019). Profile 1 was lead along the valley axis, crossing the main travertine mound (accumulation), where the paleolake was dammed (Figs. 3 and 4). Profile 2 crossed the valley perpendicular to profile 1, across the dam. Profile 3 crossed the eastern side of the valley floor and the travertine dam. Profile 4 crossed the western side of the valley floor and another travertine mound situated on a mild slope west of the travertine dam. Two transversal profiles, 5 and 6, were taken 20 m and 100 m distance from the travertine dam. Profiles 2, 3, 5, and 6 intersected profile 1 at 85 m, 137 m, 192 m and 285 m (Fig. 3), respectively.

3.3. ^{14}C dating

AMS ^{14}C dating was processed at the Center for Applied Isotope Studies at the University of Georgia, USA. For radiocarbon dating, 14 terrestrial plant macrofossils and 3 terrestrial mollusc shells were used (see Supplementary Information, Table 1). Pre-treatment and processing protocols for radiocarbon dating can be found on CAIS's webpage (http://cais.uga.edu/analysis_ams.html). Obtained ^{14}C dates were calibrated and an age-depth model was created using Oxcal 4.2.4 (Bronk Ramsey, 2009) and the IntCal13 atmospheric curve (Reimer et al., 2013).

3.4. Plant macrofossil and mollusc analysis

For plant macrofossil and mollusc analysis, sediments were sub-sampled at 3 cm (volume 40 mL) resolution, and rinsed through a 200 μm mesh. Subsequently, both plant and mollusc macrofossils were manually sorted from the residuum, identified and counted under a dissecting microscope at 12× magnification and higher. The Reference collection at the Department of Botany, Charles University was consulted for identification of plant remains together with several atlases and identification keys (Bojňanský and Fargašová, 2007; Cappers et al., 2006; Berggren, 1969; Katz et al., 1977; Velichkevich and Zastawniak, 2006, 2008). Plant nomenclature follows Kubát et al. (2002). Molluscs were identified using Ložek (1964), Horsák et al. (2013, 2019) and Nekola et al. (2018).

3.5. Pollen analysis

For pollen analysis, sediments were sub-sampled every 6 cm (volume 1 cm^3). The samples were later processed following standard techniques that use HF and HCl to eliminate mineral material from the samples (Faegri et al., 1989). A minimum of 500 terrestrial pollen grains were identified except between 947 and 793 cm (i.e. the inorganic basal part of profile) where a total of 300 pollen grains were counted. Pollen identification was aided by standard keys and photo collections (Beug, 2004; Reille, 1992; Punt and Clarke, 1984; Blackmore et al., 2003). Non-pollen palynomorphs were identified following Van Geel et al. (1980). Pollen counts were transformed into percentages using the sum of all terrestrial plants except *Alnus*, aquatic pollen and non-pollen palynomorphs. The excluded taxa were calculated as the proportion of the sum of all pollen grains counted in a sample.

3.6. Chironomid analysis and mean July air temperature reconstruction

For chironomid analysis, sediments were sub-sampled every 3 cm between depths 935–700 cm. Samples (1.9–18.4 g of wet weight; 1.2–13.9 g of dry weight) were deflocculated for 20 min in 10% KOH (60–75 °C) and then passed through 250 and 100 μm mesh sieves. Sediments with at least 6 g of dry weight were mostly processed. At depth 905 cm, the density of chironomid heads were $<10\ g^{-1}$, thus a larger volume was sorted. Chironomid capsules

were hand-sorted under a dissecting microscope (20–40× magnification), and only specimens consisting of more than half of the mentum were counted. Chironomid heads were standardized to 1 g of dry sediment (sediment was dried to a constant weight at 105 °C). Chironomids were identified to standardised types following Brooks et al. (2007). A minimum number of 35 head capsules were counted (with the exception of depth 811 cm, where 20 head capsules were counted), and the recommended count of 50 capsules was reached in more than 50% of the samples. This is recommended for calculating and reconstruction July mean air temperatures (T_{July}) (Heiri and Lotter, 2001; Quinlan and Smol, 2001). Selected chironomid taxa were classified into ecological categories according to requirements regarding lake trophic status, bathymetric distribution and preference for macrophytes (Wiederholm, 1983; Brooks et al., 2007). At depths 820–814 cm, 844–832 cm, and 935–883 cm, chironomid abundances were relatively low, thus samples were merged (taken as a one depth) to reach a sufficient number of head capsules necessary to reconstruct T_{July}. Three samples (depths 893 cm, 871 cm and 790 cm) were excluded due to the absence of head capsules. A total of 14 depths from 33 sorted samples were therefore used to reconstruct past T_{July}. For temperature reconstruction a chironomid-temperature inference model based on a Swiss-Norwegian chironomid calibration dataset and Weighted-Averaging/Partial-Least-Squares regression was used (Heiri et al., 2011). The model is characterized by a bootstrapped (cross-validated) root mean squared error of prediction (RMSEP) of 1.4 °C and r^2 of 0.87 (Heiri et al., 2011) when assessed within the calibration dataset. Inferred T_{July} values were adjusted to 0 m asl of modern sea level using a lapse rate of 0.6 °C/100 m (see e.g. Heiri et al., 2014a) for comparisons with other reconstructions (Heiri et al., 2014b). Percentages were square-root transformed before reconstruction. Chironomid-based palaeotemperature reconstructions in the northern hemisphere are conventionally calibrated to July or August temperature, which represent the warmest month of the year in large parts of the Northern Hemisphere, although chironomid assemblages can be expected to respond mainly to changes in absolute temperatures during the multi-week period of maximum temperatures during summer, rather than to temperatures during a particular month (Samartin et al., 2017). Reconstructed T_{july} can be expected to be closely correlated to past changes in such absolute summer temperature values and to be representative for past temperatures during July as the month is defined by Berger and Loutre (1991; i.e. a constant number of days from Spring equinox).

3.7. Geochemical and sedimentological analyses

Loss-on-ignition (LOI) was used to determine the amount of organic carbon and carbonates present in the sediments (Heiri et al., 2001). One cm^3 samples were dried at 105 °C for 24 h, ground up and weighed to calculate water content. Samples were then dried at 550 °C and 950 °C, each for 3 h, and then weighed to determine percent organic carbon and carbonate content.

Magnetic susceptibility (MS) provides information about the amount of transported clastic material caused by erosion (Karlén and Matthews, 1992; Shakesby et al., 2007), and was determined using a Kappabridge KLY-2 magnetic system (Agico, Czech Republic). The instrumental data were normalized to obtain mass-specific magnetic susceptibility in $m^3 \cdot kg^{-1} \cdot 10^{-9}$.

Samples for geochemical analysis were dried and ground up to reduce sediment heterogeneity. Geochemical composition of the sediments was determined using a pXRF Innov X Delta device with a 4W Rh tube and 25 mm 2 silicon drift detector in soil analysis mode (each measurement consists of two 30-s beams). Values below the detection limit were replaced by values equivalent to half of the instrumental detection limit. For results, see the Supplementary Information.

3.8. Stable isotope analyses

Stable carbon isotope analysis was performed on carbonate fragments manually collected from the wet-sieved sediment. If the carbonate sand was very fine and did not allow manual separation, the wet sieved sediment was dried and leached with 30% H_2O_2 to remove organic carbon from the sample. Isotope relative mass spectrometry (IRMS) was used to determine the abundance of carbon and oxygen stable isotopes using the same method as Juřičková et al. (2018). Briefly, carbon dioxide was released from carbonates with anhydrous phosphoric acid; then it entered a mass spectrometer (Deltaplus XL, Thermo Finnigan, Bremen, Germany) via an interface (GasBench II, Thermo Finnigan, Bremen, Germany). The relative abundances of $^{13}C/^{12}C$ and $^{18}O/^{16}O$ found within the released carbon dioxide molecules were expressed using a 'δ' notation. Standard deviations for both $^{13}C/^{12}C$ and $^{18}O/^{16}O$ were mostly <0.2‰. Final results were expressed with respect to the International Atomic Energy Agency (IAEA) standard VPDB (Vienna Pee Dee Belemnite; IAEA, Vienna, Austria).

3.9. Numerical analyses and data visualization

Summary diagrams containing geochemical, macrofossil, mollusc, pollen and chironomid data were created in Tilia v. 1.7.16 and TILIA.GRAPH (Grimm, 2011). Cluster analysis by sum-of-squares (Coniss analysis) was applied to identify the main zonation of the local (macrofossil, mollusc, chironomid and geochemical analysis) and regional (pollen) successions.

To explore temporal patterns within each of the datasets, principal components analysis (PCA) (geochemical composition, pollen data) and detrended correspondence analysis (DCA) (macrofossil and mollusc data) were performed using Canoco v 5.10. (Ter Braak and Šmilauer, 2012) with a down-weighting of rare species, logarithmic transformation of species data and detrending by segments. A gradient length of 1.8 standard deviation units (SD) was identified for pollen, 1.6 SD units for geochemical composition, 10.5 SD units for macrofossils and 7.8 SD units for molluscs. For pollen, 25.58% of the variation is explained by the first axis, 58.98% for geochemical composition, 9.96% for macrofossils and 17.64% for molluscs.

A combined diagram with both $\delta^{18}O$ (VPDB) and $\delta^{13}C$ (VPDB) values was created in Canoco v 5.10. (Ter Braak and Šmilauer, 2012).

4. Results

4.1. Sedimentological analysis

The bottom section of the sediment profile (947–783 cm) consisted predominantly of inorganic calcareous sediment often with rounded travertine pieces and sand. Sediment between 783 and 686 cm was more fine-grained with an admixture of organic limnic sediment (gyttja) and fine travertine pieces. Sediments alternated between dark brown organic layers and beige inorganic calcareous layers between depths 686 and 638 cm. Consolidated travertine was present between 638 and 590 cm. Highly organic material with fine travertine pieces gradually changed to light beige calcareous sediment between 590 and 560 cm. Organic sediment was again present between 406 and 400 cm. Inorganic sediment continued from depth 406 cm to the top of the profile (0 cm). For a more detailed description, see Table 2 in the Supplementary Information.

4.2. Radiocarbon dating

A reliable age-depth model was obtained using 13 AMS radiocarbon dates (SI Table 1) (Fig. 2), which reached an agreement value of 81% between calibrated and modelled values. The margin of error of the modelled ages (95% confidence interval) varied mostly between 89 and 384 years (935–838 cm), 76 and 150 years (837–688 cm), 200 and 274 years (590–582 cm) and 52 and 200 years (582–401 cm). Four radiocarbon dates were excluded from the age-depth model (SI Table 1); samples UGAMS 24859 and UGAMS 29463 were much younger than neighbouring data indicating contamination by younger material from the upper section of the profile between 686 and 643 cm. This was probably caused by breaking through the consolidated travertine layer (between 643 and 590 cm) during coring; and UGAMS 29465 and UGAMS 29466 were excluded as they are present in clayey flushes (333–0 cm) with evident sediment mixing where superposition of layers was not maintained.

4.3. ERT survey

Profile 1 (the longitudinal profile; 0–555 m length, almost 100 m depth) had four distinct resistivity zones (Fig. 4). Clearly identifiable was the travertine body located approximately 100–150 m from the start of the profile, reaching a thickness of approximately 18–20 m. The travertine deposit appeared to be represented by sharply limited zones of high resistivity (mostly 200–800 Ωm with extremes above 1000 Ωm). Approximately 150 m from the start of the profile, a 10–12 m thick surficial zone of medium resistivity (10–30 Ωm) was observable along the whole length of the profile, which was interpreted as travertine enriched lake sediment or lake/swamp sediments. A zone of low resistivity (3–10 Ωm) dominated between 5–10 m and 25–30 m below the surface along the whole profile, interpreted to be the original floodplain deposits. The bottom 30–100 m of the profile was formed by distinct zone of about 30–80 Ωm interpreted as a bedrock. Between 170 and 180 m from the start of the profile 1 at a depth 30–45 m was a significant vertical step (~10 m) in two distinct resistivity zones, indicating presence of a tectonic fault transversal to the valley. This is supported by the presence of travertine mounds, formed by springs, which are found roughly in line of the presumed faultline. The top 10–15 m of profile 2 were dominated by medium resistivity (Fig. 4), with distinct isolated islands of high resistivity (200–500 Ωm) interpreted as travertine bodies. Below 15 m from the surface, a low resistivity zone (3–10 Ωm) interpreted to be the original floodplain extends to a depth of 35–45 m below the surface. Bedrock exists below the original floodplain and had a medium resistivity (30–80 Ωm). According to profile 3 (Fig. 4), a 40 m-long, 40 m-wide and approximately 18 m tall compact travertine dam occurred, running east to west. Under the high-resistivity travertine body, a low resistivity zone existed until the bottom of the profile. The western end of profile 4 (approximately 50 m from the start of the profile) was formed by high-resistivity travertines, while the eastern side had medium resistivity of 30–50 Ωm (Fig. 3). The resistivity of two transversal profiles 5 and 6 was practically identical (Fig. 4). The top 5–10 m was formed by a medium resistivity (15–30 Ωm) layer, with a low (3–10 Ωm) resistivity zone below 10 m extending to approximately 30–35 m where the resistivity again increased to 20–60 Ωm.

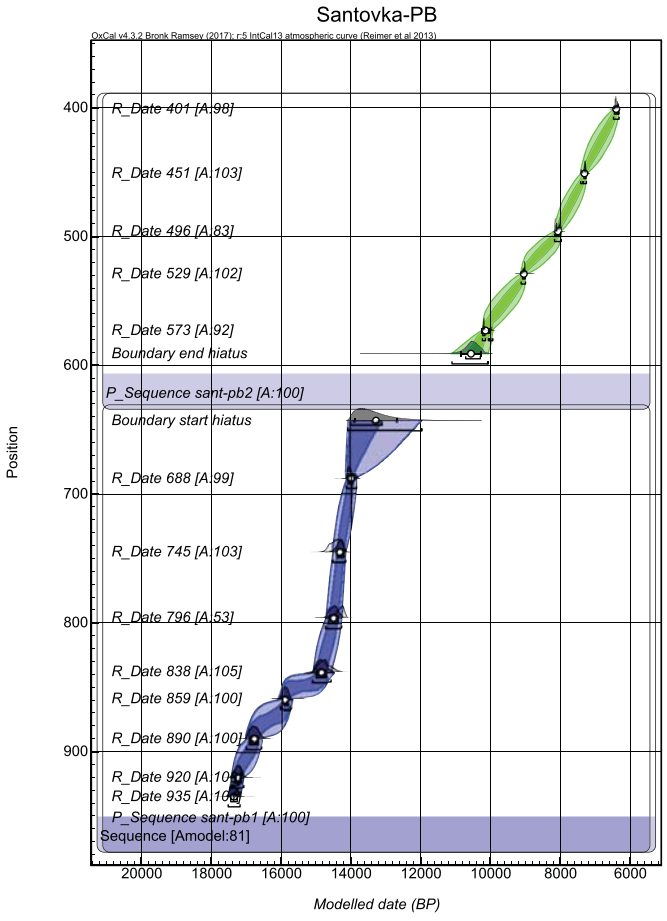

Fig. 2. Age-depth model of Santovka-Pramene Budzgov based on 13 ^{14}C dates. Highest posterior density ranges of 95.4% (light green colour) and 68.2% (dark blue colour) are displayed. Between 638 and 590 cm a temporal hiatus in fossil record was present. (For interpretation of the references to colour in this figure legend, the reader is referred to the Web version of this article.)

4.4. Stable isotopes

δ^{13}C values that span the end of MIS 2 (depth 947–803 cm; 17,540–14,560) varied dramatically (ranging between −7.642‰ and +7.947‰), likely due to high erosion rates and the accumulation of diverse sedimentary material from the surrounding vicinity. δ^{18}O values ranged from −8.544 to −5.573 during the MIS 2. All Lateglacial samples (depth 803–686 cm; 14,560–13,950 cal BP) and six samples of early Holocene age (depth 591–550 cm; 10,560–9570 cal BP) had very high values of δ^{13}C (range from +0.2 to +7.1), which coincide well with isotope data from Slovakian travertines analysed by Gradziński et al. (2008), where δ^{13}C values range from +0.9 to +8.4‰ (Fig. 5). Lateglacial δ^{18}O values ranged from −10.739 to −6.913. The remaining samples of Holocene age (depth 547–472; 9500–7660 cal BP) showed distinctly lower δ^{13}C values (range from 0‰ to −2‰), while δ^{18}O showed a slight shift to higher values ranging from −7.632‰ to −6.254‰.

4.5. Macrofossils

Zone SA-mal, the bottom-most section of the sediment profile (depth 947–876 cm; 17,540–16,360 cal BP) was marked by a mixture of dwarf shrubs and herbs (*Betula nana*, *B. humilis*, Poaceae, *Selaginella selaginoides*), which indicate the presence of dwarf-birch tundra vegetation around the coring site (Fig. 6). Fish remains, *Zannichellia palustris* and *Cenococcum geophilum* (indicator of soil erosion in lake sediments) point to the existence of a stream at the coring site, which was also confirmed by higher values of MS. Zone SA-ma2 (depth 876–803 cm; 16,360–14,560 cal BP) was

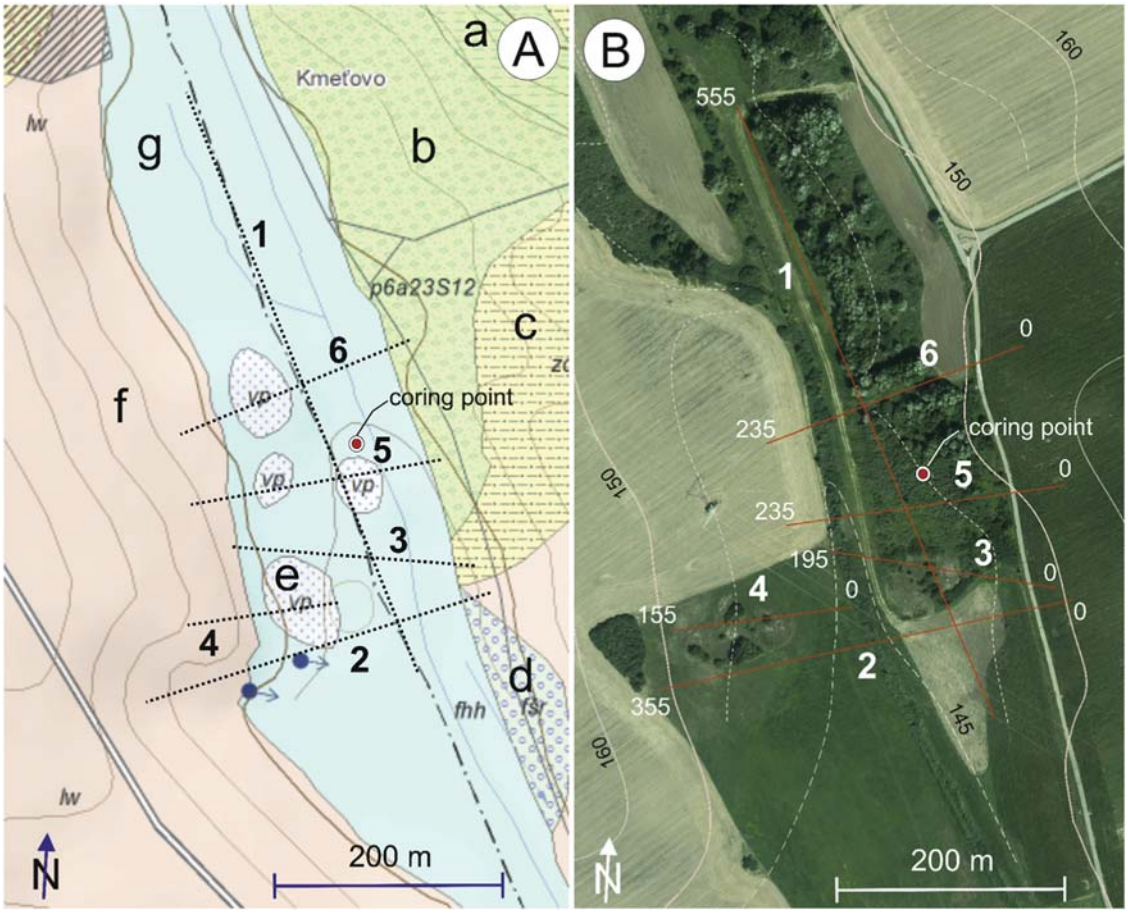

Fig. 3. Position of the Electrical Resistivity Tomography profiles (1–6) measured in the study area. A: Geological basemap 1:50 000 (Nagy et al., 1998); a – tuffitic sandstones and andezite conglomerates; b – epiclastic andesitic sandstones; c – eluvial-deluvial sediments; d – fluvial sediments of fluvial terrace; e – travertine; f – aeolian sediments (loess, loess loam); g – fluvial sediments of floodplain. B: Aerial photo of study area with contourlines (black numbers). White numbers indicate the number (large) and length (small) of each of the 6 profiles, with 0 delineating the start of each profile. Red dot indicates location of the coring point. (For interpretation of the references to colour in this figure legend, the reader is referred to the Web version of this article.)

characterized by an increase in species richness of aquatic macrophytes (e.g. *Stuckenia filiformis*, *Hippuris vulgaris*, *Potamogeton pussilus* agg.), which may indicate the transition from a wild stream to a permanent and calmer stream flow. Terrestrial vegetation was still predominately birch-dwarf tundra vegetation but with a higher representation of herbs (e.g. *Chenopodium glacum/rubrum*, *Polygonum aviculare*, *Veronica/Pseudolysimachion*), and less grasses in comparison to the previous zone. In Zone SA-ma3 (depth 803–686 cm; 14,560–13,950 cal BP), numerous new plant taxa rapidly appeared, especially wetland (e.g. *Carex caespitosa*, *Cicuta virosa*, *Sparganium erectum*, *Schoenoplectus tabernaemontani*) and aquatic species (*Potamogeton crispus*, *Chara* sp.), indicating the development of a calcareous, nutrient rich water reservoir with stagnant or slowly flowing water. The reservoir had to be deep enough to allow the presence of fish stock. Dwarf shrub vegetation still dominated with an admixture of *Pinus sylvestris/mugo*. Between 686 and 591 cm, a hiatus in fossil record was present. Above the hiatus in Zone SA-ma4 (depth 591–550 cm; 10,560–9570 cal BP), relatively few macrofossils were found, except *Schoenoplectus tabernaemontani* and *Chenopodium glaucum/rubrum*. Fish remains and *Chara* sp. oogonia together with low MS values and high organic and carbonate content indicate the presence of a shallow calcareous pool. In the upper zone of SA-ma5 (depth 550–480 cm; 9570–7800 cal BP) only a few macrofossils were preserved as a result of high carbonate precipitation rates of travertine deposits. Contrary, Zone SA-ma6 (depth 480–400 cm; 7800–6400 cal BP) was marked by a high abundance of macrofossils from various environmental groups. The common presence of *Chara* sp., *Najas marina*, *Ranunculus* subgen. *Batrachium*, *Schoenoplectus tabernaemontani*, *Typha latifolia/angustifolia*, *Cladium mariscus*, *Rumex maritimus*, fish remains and *Daphnia magna* ephippia point to the existence of a permanent calcareous pool surrounded by species-rich wetland vegetation. Preservation of macrofossils in the uppermost zone, SA-ma7 (depth 400–335 cm; 6400–? cal BP) was strongly influenced by increased erosional processes from the adjacent loess slopes. The presence of field weeds *Hyoscamus niger* and *Fumaria officinalis* in the profile was most likely linked with agricultural activities of Neolithic people, who may have cultivated crops on adjacent loess slopes, resulting in higher erosion rates.

4.6. Molluscs

The mollusc record covers the time interval between 14,560 and ~6000 cal BP as the bottom section of the profile (SA-mo1; depth 947–803 cm; 17,540–14,560 cal BP) was not suitable for shell preservation (Fig. 7). In general, mollusc record was very rich, consisting of 63 species identified among 7686 analysed shells. Only a single shell of the land snail *Vertigo genesii*, a cold adapted calcareous spring specialist, was found at a depth 945 cm (~17,500 cal BP). This characteristic species of the Late Glacial has

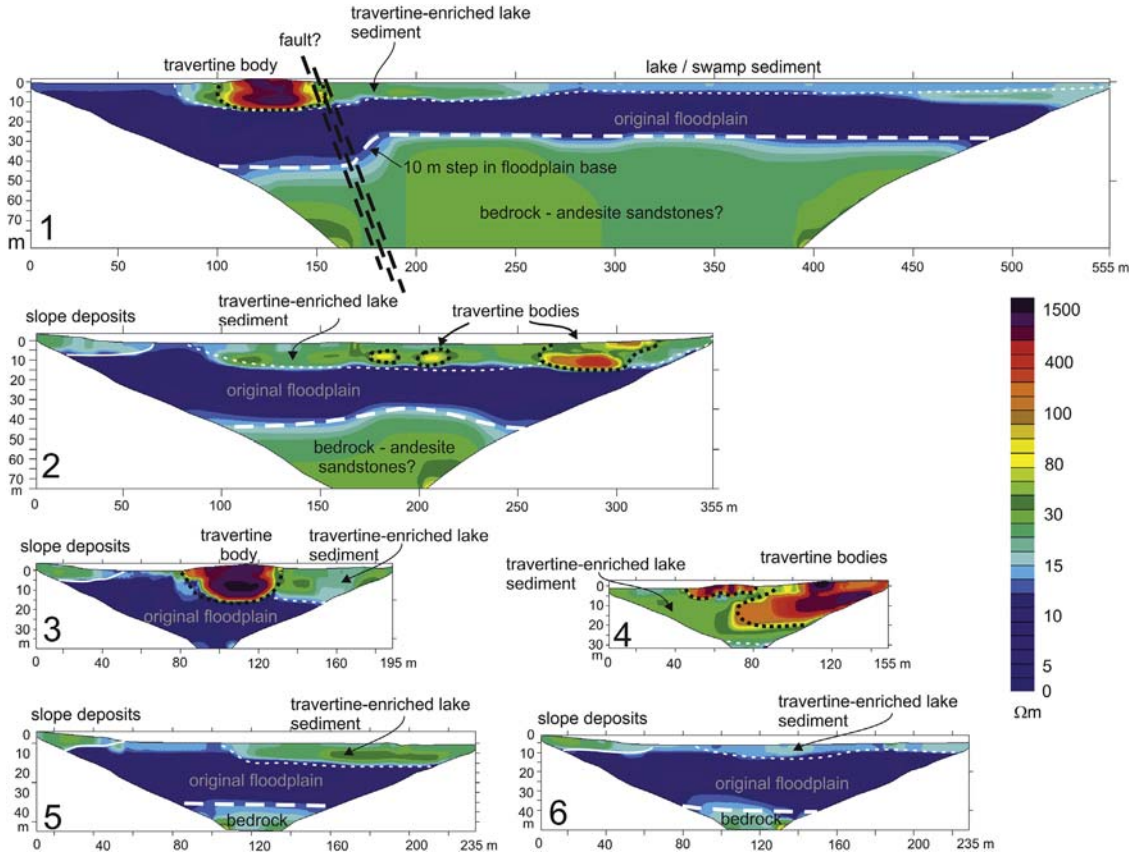

Fig. 4. Geomorphological and geological features of the Santovka-Pramene Budzgov valley based on interpreted Electrical Resistivity Tomography profiles (1–6). 1) is the longitudinal profile; 2–6) are the transversal profiles.

only rarely been reported from the full glacial layers. During Zone SA-mo2 (depth 803–686 cm; 14,560–13,950 cal BP), steppe snail species *Granaria frumentum* and *Helicopsis striata*, and the characteristic steppe-tundra snail *Vallonia tenuilabris* that became extinct in Europe during Early Holocene clearly indicate cold steppe conditions. Spring fen species (*Pupilla alpicola* and *Vertigo geyeri*) suggest the presence of fen habitats, likely developed along spring brooks. Except several species of shallow pools, running-water mollusc species were common, including *Pisidium tenuilineatum* and *P. pulchellum*; the latter represents the first record in Slovakia from both past and present Quaternary. Between depths 686–591 cm (13,950–10,560 cal BP), a 3000-year long hiatus was recorded in which the site became notably drier, without any running water habitats. During Zone SA-mo3 (depth 591–550 cm; 10,560–9570 cal BP), *Granaria frumentum* and *Pupilla muscorum* indicate an open, dry steppe environment, while the fen snails *Vertigo angustior* and *Pupilla alpicola*, and aquatic snails *Anisus vorticulus* and *Bathyomphalus contortus* show combination of fen wetland with shallow pools. A clear developmental shift to a typical semi-dry fen without any aquatic habitats, but also any steppe habitats in the surroundings, was observed at the beginning of Zone SA-mo4 (depth 550–480 cm; 9570–7800 cal BP). In contrast, a strong moistening happened at the beginning of Zone SA-mo5 (depth 480–400 cm; 7800–6400 cal BP) as most several land snail species disappeared (e.g. *Vertigo pygmaea*) or sharply reduced their abundances (e.g. *Vallonia pulchella*). These were replaced by a rich assemblage of aquatic molluscs requiring stable standing waters (e.g. *Anisus vorticulus* and *Lymnaea stagnalis*). Two wetland species, *Vertigo antivertigo* and *V. moulinsiana*, were abundant also in the wettest period (i.e. around 6400 cal BP) as they can climb up the vegetation and thus survive even long periods of habitat overflooding. In Zone SA-mo-6 (depth 400–335 cm; 6400–? cal BP), only few mollusc shells were found.

4.7. Pollen

Vegetation in Zone SA-p1 (depth 947–885 cm; 17,540–16,600 cal BP) was typical of cold, glacial conditions, dominated by non-forest vegetation (e.g., Poaceae, *Artemisia, Helianthemum nummularium* t.) and open stands of undemanding trees and shrubs such as *Pinus sylvestris* t., *P. cembra*, *Larix*, *Juniperus*, *Betula pubescens* t., and *B. nana* t. Pollen of deciduous trees (*Quercus, Corylus avellana*, *Tilia*, *Ulmus*) sporadically occurred as well (Fig. 8). Pollen grains of a tertiary species, *Carya*, were found in depths 929 (2 grains) and 935 (1 grains) cm. At the onset of Zone SA-p2 (depth 885–772 cm; 16,600–14,410 cal BP), *Pinus sylvestris* t. expanded synchronously with a decline in Poaceae and slight increase in *Quercus*, *Corylus avellana, Sparganium* and Cyperaceae indicating a change in local hydrological conditions. The composition of forest vegetation remained the same until the beginning of Zone SA-p3a (depth 772–686 cm; 14,410–13,950 cal BP), when cold-adapted vegetation disappeared (*Pinus cembra*, *Dryas* sp.) and/or gradually declined (*Larix*, *Betula nana* t.), and was replaced by the rapidly increasing *Pinus sylvestris* t. Aquatic and wetland plants (*Sparganium/Typha angustifolia*, *Typha latifolia* t., *Potamogeton/Triglochin*) also expanded during this zone indicating a change in hydrological conditions. Between 686 and 591 cm, a sediment hiatus is present. After the hiatus, in Zone SA-p3b (depth 591–573 cm; 10,520–10,140 cal BP), the pollen record remained the same as in the previous zone. The most prominent change in vegetation cover

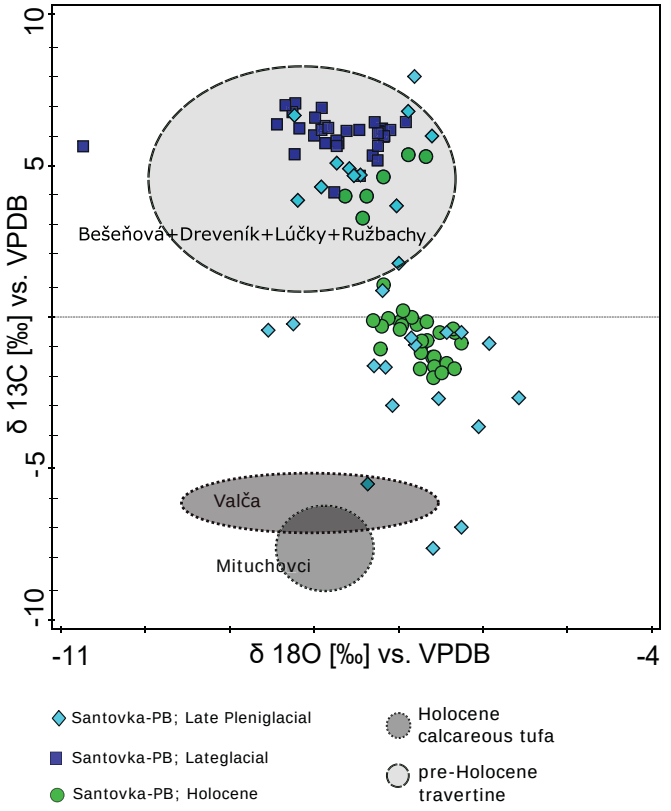

Fig. 5. Comparison of stable $\delta^{13}C$ and $\delta^{18}O$ isotopes derived from carbonate samples from Santovka-Pramene Budzgov and other sites from Slovakia (their locations indicated in Fig. 1). Data sources: Bešeňová+Dreveník + Lúčky + Ružbachy (Gradziński et al., 2008); Valča (Juřičková et al., 2018); Mituchovci (Dabkowski et al., 2019).

occurred at the onset of Zone SA-p4 (573–480 cm; 10,140–7800 cal BP) when deciduous trees (*Quercus*, *Corylus avellana*, *Tilia*, *Ulmus*) rapidly expanded, as did *Picea abies*. In Zone SA-p5 (480–400 cm; 7800–6400 cal BP), late-successional trees (*Fagus sylvatica, Abies alba*, *Carpinus betulus*) continuously occurred in the pollen record, and wetland taxa (*Typha latifolia* t. *Pediastrum boryanum* agg., *P. integrum*) increased indicating a change in local hydrological conditions. Additionally, crops (*Triticum* t.) and ruderals (*Polygonum aviculare* t.) first appeared ~7260 cal BP during this zone which overlaps with the Middle Neolithic period. Vegetation in Zone SA-p6 (depth 400–0 cm; 6400–? cal BP) is characterized by an increase in non-forest vegetation (e.g. Chenopodiaceae (Amaranthaceae), Poaceae) and the continuous occurrence of crops and ruderals, indicating increasing agricultural areas.

4.8. Chironomids

Zone SA-chi1 (depth 935–883 cm; 17,360–16,560 cal BP) was characterised by very low chironomid abundances (see chironomid productivity – i.e. head capsules per 1 g of dry sediment, Fig. 9). Phytophilic and epilithic chironomids (*Paratanytarsus* sp., *Cricotopus intersectus/laricomalis* t., *Orthocladius* sp.), as well as semi-terrestrial genera (*Limnophyes*|*Paralimnophyes*, *Pseudosmittia* sp.) were present, which are all indicative of a shallow lake with macrophytes in the littoral. In Zone SA-chi 2 (depth 883–844 cm; 16,560–15,150 cal BP), where low densities of chironomids continue, semi-terrestrial *Pseudosmittia* sp. again occurred together with several phytophilic and epilithic taxa, which were also recorded in the Zone SA-chi1. However, the appearance of *Odontomesa fulva* t., a cold stenotherm indicative of running water, and taxa preferring deep profundal zones (*Micropsectra contracta* t., *Zalutschia* sp.) suggest the input of cold running water from a nearby stream and increasing water depths. Zone SA-ch3 (depth 844–832 cm; 15,150–14,780 cal BP) taxa (*Chironomus plumosus* t.,

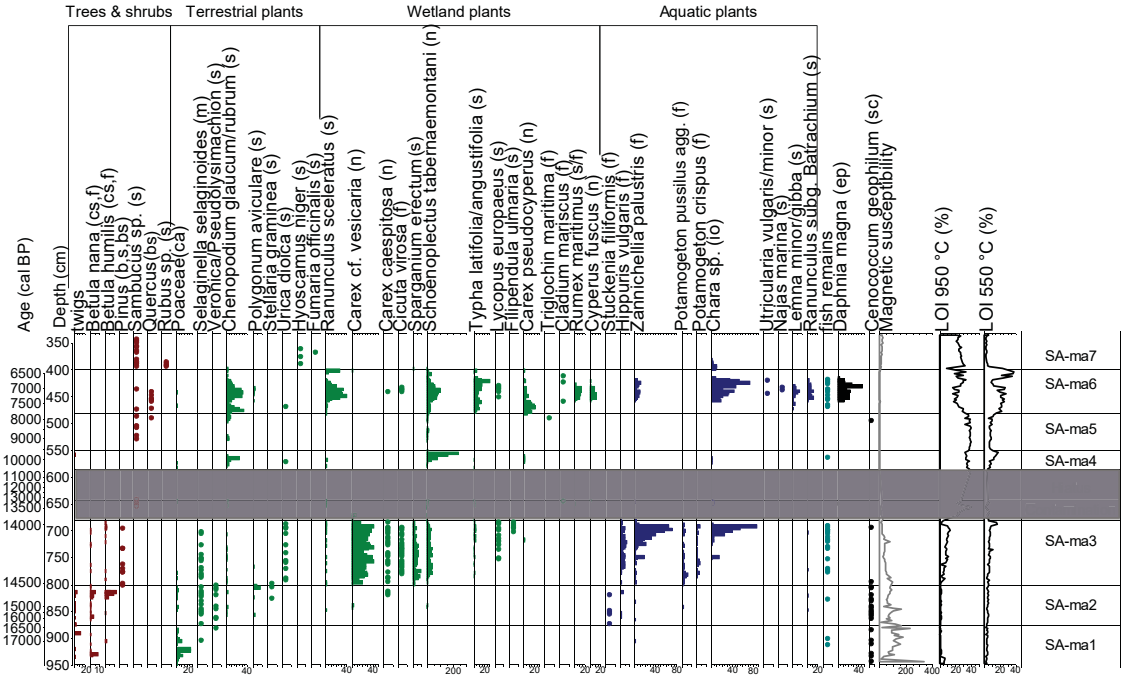

Fig. 6. Simplified macrofossil concentration diagram with loss on ignition and magnetic susceptibility from Santovka-Pramene Budzgov plotted on depth (cm) and calibrated age scales (years Before Present). Concentrations are represented by 40 cm^3 of sediment. b = bud; bs = bud scale; cs = catkin scale; ep = ephippium; f = fruit; n = nutlet; s = seed; sc = sclerotium. Colours define major vegetation groups (i.e. trees and shrubs, terrestrial plants, wetland plants, and aquatic plants). Grey box indicates the presence of a sediment hiatus. Analyst A. Šolcová. (For interpretation of the references to colour in this figure legend, the reader is referred to the Web version of this article.)

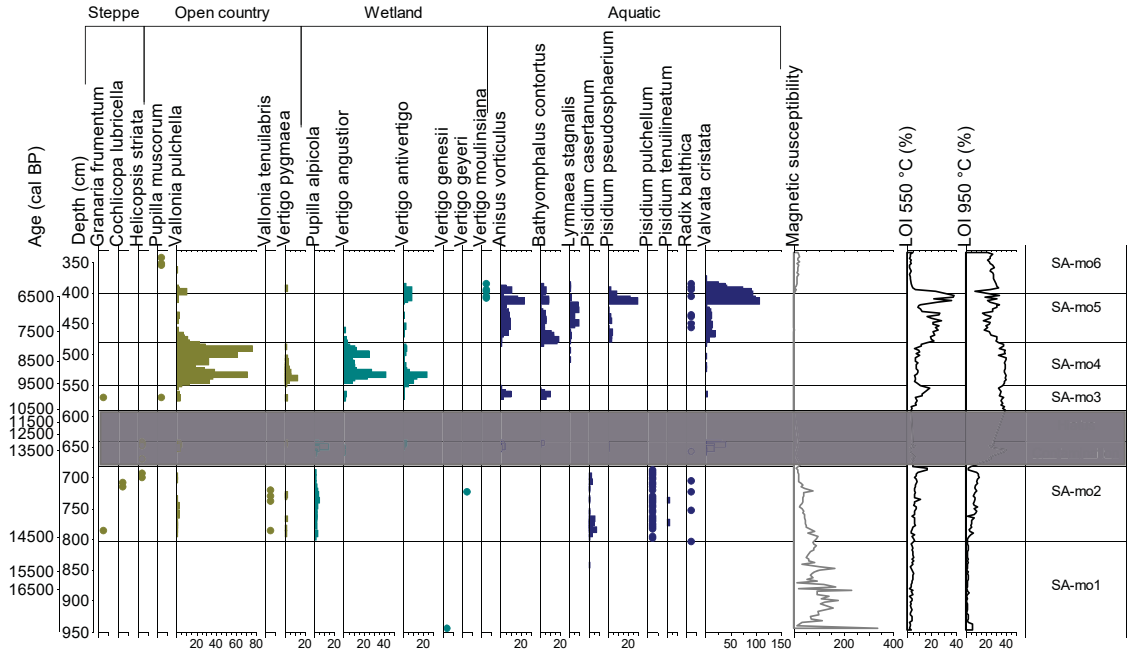

Fig. 7. Simplified mollusc concentration diagram with loss on ignition and magnetic susceptibility from Santovka-Pramene Budzgov plotted versus depth (cm) and calibrated age (years Before Present). Concentrations are represented by 40 cm^3 of sediment. Colours define dominant mollusc groups (i.e. steppe taxa, open country taxa, wetland taxa, and aquatic taxa). Grey box indicates the presence of a sediment hiatus. Analyst M. Horsák. (For interpretation of the references to colour in this figure legend, the reader is referred to the Web version of this article.)

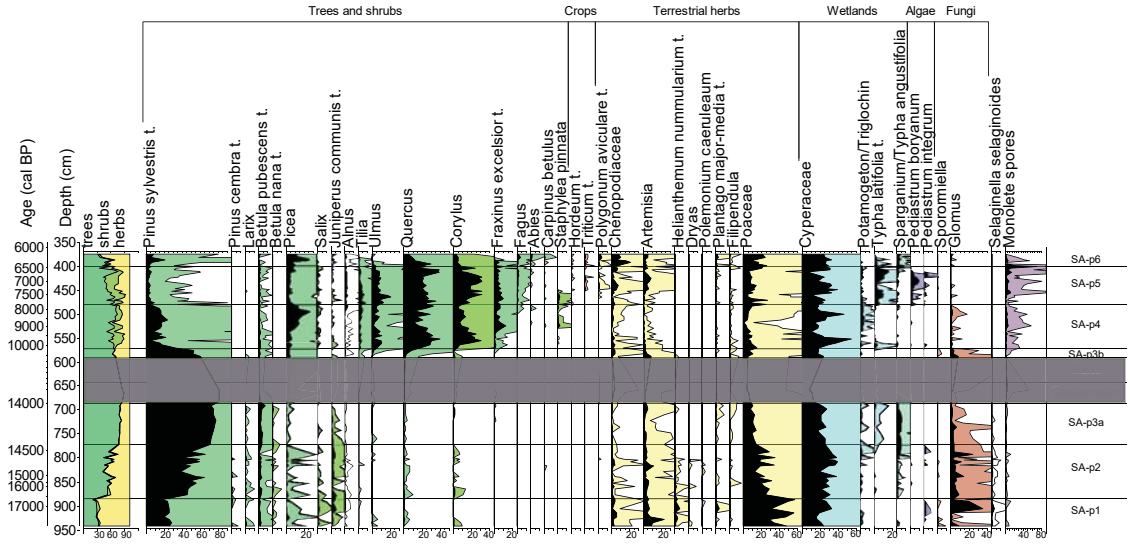

Fig. 8. Simplified percentage pollen diagram from Santovka-Pramene Budzgov plotted on depth (cm) and calibrated age scales (years Before Present). Colours represent major vegetation groups (i.e. trees and shrubs, crops, terrestrial herbs, wetland taxa, algae and fungi). Grey box indicates the presence of a sediment hiatus. Analyst E. Jamrichová. (For interpretation of the references to colour in this figure legend, the reader is referred to the Web version of this article.)

Microtendipes pedellus t.) are indicative of higher trophic status and finer substrates. The input of flowing water was reflected by typical lotic taxa (*Parametriocnemus*/*Paraphenocladius* sp. or *Odontomesa fulva* t.), but the occurrence of profundal taxa such as *Micropsectra contracta* t. and *M. insignilobus* t. (sensu lato) could indicate higher water depth. Zone SA-chi 4 (depth 832-802 cm; 14,780–14,550 cal BP) was characterised by the presence of typical taxa of running water (*Odontomesa fulva* t. and *Parametriocnemus*/*Paraphenocladius* sp.), as well as semiterrestrial (*Pseudosmittia* sp., *Limnophyes*/*Paralimnophyes* sp.) and phytophilic/epilithic taxa (*Orthocladius* sp., *Cricotopus cylindraceus* t.). Cold stenotherm species (*Micropsectra radialis* t.) and oligostenotherms species (*Apsectrotanypus* sp.) were found in this zone, signalling the coldest conditions of the entire profile. Zone SA-ch5 (depth 802–700 cm; 14,550–14,070 cal BP) was characterised by an increase in chironomid density and taxonomic diversity, indicating an increase in lake productivity. Taxa preferring moderate to high temperatures, higher trophic states and macrophytes were frequent in this zone (*Cricotopus* sp., *Phaenopsectra flavipes* t., *Chironomus plumosus* t.). Increase of temperature was probably accompanied by a higher water table (higher representation of taxa that can colonize deeper lakes such as *Micropsectra contracta* t., *M. insignilobus* t.).

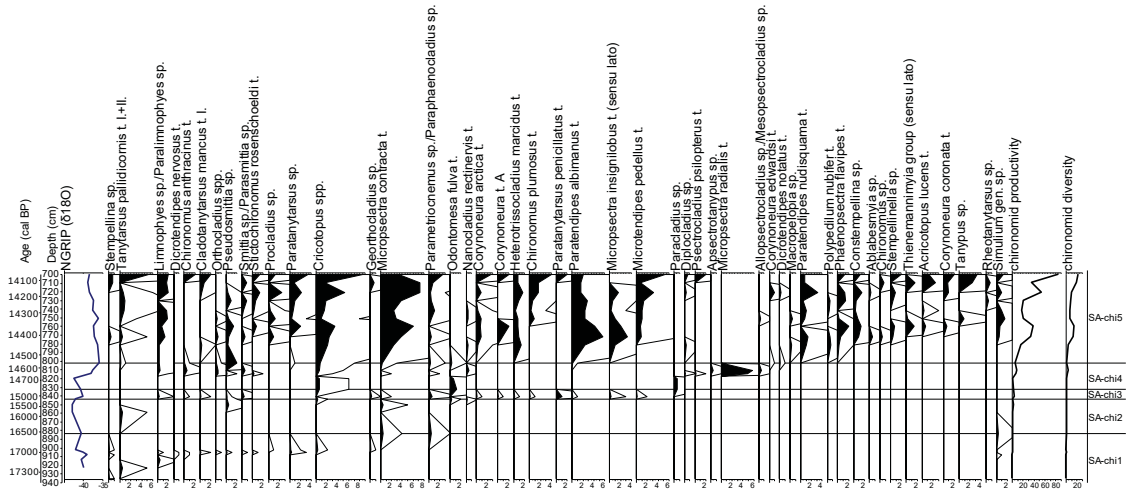

Fig. 9. Simplified chironomid concentration diagram of the most important and abundant chironomid morphotypes from Santovka-Pramene Budzgov plotted on a depth (cm) and the calibrated age scale (years Before Present). Concentration values are represented by their density per gram of dry weight. Some rare groups were merged into wider species complexes or to genus level for illustration purposes, but not for the quantitative T_{july} reconstruction. NGRIP $\delta^{18}O$ data (NGRIP dating group, 2006) were downloaded from ftp://ftp.ncdc.noaa.gov/pub/data/paleo/icecore/greenland/summit/ngrip/gicc05-20yr.txt. Chironomid productivity (head capsules per 1 g of dry sediment) together with chironomid diversity (number of taxa per 1 g of dry sediment) are shown on the right side of the diagram. Analyst P. Pařil.

4.9. Chironomid based temperature reconstruction

During the end of MIS 2 (~17,040–15,250 cal BP), T_{july} temperatures ranged between 15.7 °C and 15.3 °C (adjusted to modern sea level), based on merging 7 samples between 935 and 883 cm and 5 samples between 859 and 832 cm (Fig. 10). However, these two merged samples should be interpreted with caution as these reconstructions did not meet the 35 head capsule minimum. A more reliable reconstruction of T_{july} began ~14,660 cal BP (by merging depths 814 and 820 cm), which indicates a temperature of 13.7 °C. At 14,620 cal BP, temperatures were 12.7 °C (811 cm) but this sample was based on 19 specimens and thus should be interpreted with caution. From 14,620 to 14,440 cal BP (depths 811 cm and 781 cm), we observed a rapid increase in T_{july} by more than 3.8 °C, from 12.7 °C to 16.5 °C. Temperatures in the remaining profile (depth 14,410–14,070 cal BP; 772–700 cm) oscillated between 14.1 and 17 °C with changes generally within the model error of 1.4 °C.

5. Discussion

5.1. Ecosystem state during MIS 2: Steppe-tundra or taiga forest?

The surrounding vegetation at Santovka-PB was dominated by grasses (more than 50%) followed by *Pinus sylvestris* (around 20%)

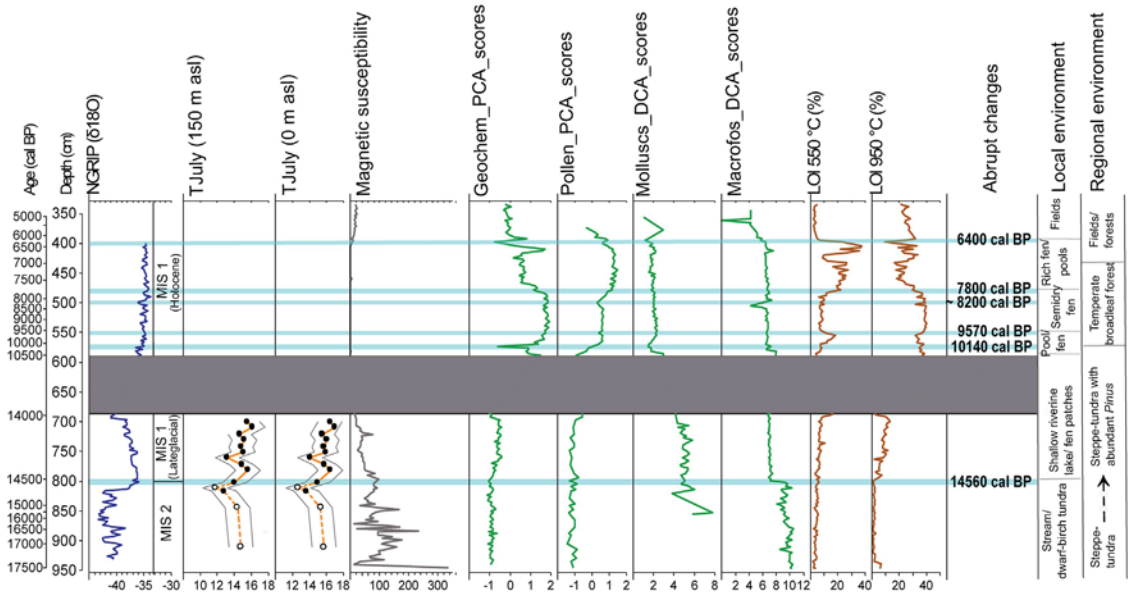

Fig. 10. Summary diagram of selected biotic and abiotic proxy data from Santovka-Pramene Budzgov (North Greenland Ice Core Project $\delta^{18}O$ values, mean July temperature (T_{July}) reconstruction based on the chironomid record, Magnetic susceptibility, PCA (Principal Components Analysis) and DCA (Detrended Correspondence Analysis) results of biotic proxy data and Loss on ignition). Displayed data were selected to demonstrate temporal changes in the local and regional environment. NGRIP $\delta^{18}O$ data (NGRIP dating group, 2006) were downloaded from ftp://ftp.ncdc.noaa.gov/pub/data/paleo/icecore/greenland/summit/ngrip/gicc05-20yr.txt. Empty circles in the T_{July} curve indicate limited validity of the reconstruction due to a low number of chironomids. Full circles display more reliable results in the T_{July} reconstruction, and are based on more than 35 individuals and a maximum of two adjoining depths merged together. Abrupt changes in the fossil record are highlighted by blue horizontal lines. Grey box indicates the presence of a sediment hiatus. (For interpretation of the references to colour in this figure legend, the reader is referred to the Web version of this article.)

and with the increased admixture of open-landscape taxa (e.g. *Artemisia* and Amaranthaceae; incl. former Chenopodiaceae) between 17,550 and 16,500 cal BP (Fig. 8), suggesting an open steppe-tundra ecosystem in the vicinity of the site. According to Chytrý et al. (2019), Central European full-glacial steppe-tundra ecosystem with loess deposition was comprised of an admixture of dry environments (i.e. mosaics of desert or typical steppe), and more mesic/wetter environments on north-facing slopes, or along streams. In our case, on the left side of the valley where loess had been deposited (Fig. 3A), a typical steppe environment dominated by perennial clumped grasses probably prevailed and a sparse tree layer of *Pinus sylvestris* may have grown on more mesic places around Santovka-PB during MIS 2. Macrofossil analysis further revealed the presence of dwarf-birch tundra, which likely existed at the bottom of the valley. Abundant macrofossils of grasses may also indicate the local proximity of wet grasslands occurring along the local stream (Fig. 6) (see SI Fig. 2 for modern analogue). Paleoecological investigations from the Pannonian Basin indicate similar results with the predominance of *Pinus* (>50% pollen) and grasses (Sümegi et al., 2011, 2013; Kustár et al., 2016), with sporadic yet significant admixtures of temperate trees (Sümegi et al., 2013). Our fossil pollen record also captured small, but continuous amounts of temperate tree pollen (*Quercus*, *Corylus avellana*, *Tilia*, *Alnus*) between 17,550 and 14,600 cal BP (Fig. 8), indicating either these species were in close proximity to Santovka-PB, or long-distance pollen dispersion. The possibility of redeposition of temperate tree pollen seems negligible in this case, as only three pollen grains of tertiary species (*Carya*) were found in the bottommost section of the profile (17,500–17,300 cal BP). Local presence of temperate trees could have occurred in gallery forests along rivers and around lakes where higher soil and air moisture aided their survival (Willis and Van Andel, 2004). Despite of presence of temperate tree pollen, we lack undeniable evidence (i.e. macrofossil, wood, charcoal) about the presence of local temperate trees during MIS 2, necessary to prove the presence of a local refugium (Tzedakis et al., 2013). In contrast to lowland sites in the Pannonian Basin, mid-elevation sites (~350–600 m asl) from the Western Carpathians indicate the presence of hemiboreal (taiga) forest (AP>80%) dominated by *Picea abies*, *Pinus* and *Betula* with an admixture of temperate trees during MIS 2 (Jankovská and Pokorný, 2008). It is hypothesized that northern temperate forest microrefugia were located there, as a result of wetter climatic conditions due to orographical precipitation and relatively higher air humidity (Ložek, 2006; Jankovská and Pokorný, 2008; Juřičková et al., 2014).

Around 16,500 cal BP (880 cm), *Pinus sylvestris* pollen increased (up to ~60%) at the expense of grasses and other open-landscape taxa, indicating the advancement of pine forests with an admixture of other conifer taxa and temperate trees (e.g. *Quercus*, *Corylus avellana*). Despite the increase in *Pinus sylvestris* pollen, the steppe-tundra ecosystem persisted. Simultaneous with the advancement of pine forests was the first appearance of aquatic macrophyte taxa (e.g. *Stuckenia filiformis*, *Hippuris vulgaris*) (Fig. 6), suggesting wetter conditions. According to Nádor et al. (2007), mean July air temperatures decreased to ~12–15 °C and dry loess steppe started to expand in the Pannonian Basin around 16,500 cal BP as humidity decreased, which is contrary to our results. Such discrepancies could be explained by local climate deviations possibly linked to the proximity of the Western Carpathians. Moreover, a short-term substantial humid pulse and/or overall climate amelioration was recorded between 15,000 and 14,800 cal BP, as indicated by *Potamogeton pussilus* agg., *Schoenoplectus tabernaemontani* and several chironomid taxa (SA-chi 3, Fig. 9) all indicating a higher water table (Fig. 6).

5.2. Biotic response to abrupt climate change at MIS 2/MIS 1 transition

An abrupt and persistent climate amelioration occurred at the MIS 2/MIS 1 transition (corresponding to the GS-2a/GI-1e transition (Lowe et al., 2008; Rasmussen et al., 2014)) around 14,640 ± 186 cal BP (GICC05 timescale). This amelioration event is well documented in the NGRIP (North Greenland Ice Core Project) oxygen-isotope record as a rapid increase in $\delta^{18}O$ indicating rising temperatures over the Greenland ice sheet (Rasmussen et al., 2006; Lowe et al., 2008). In Central Europe, this transition is generally considered to coincide with the Oldest Dryas to Bølling-Allerød transition apparent in many lacustrine sediment records (e.g. Van Raden et al., 2013). This climatic event was captured at Santovka-PB, based on chironomid and macrofossil record, and is dated to 14,560 ± 130 cal BP (803 cm), which is within the margin of error of the GICC05 timescale model given by Rasmussen et al. (2006) and/or within the margin of error in our age-depth model, so we believed that this climate transition occurred synchronously at Santovka-PB and in Greenland.

At the MIS 2/MIS 1 transition, chironomid-based July temperature reconstructions from other mainland sites in Europe increased between 3 and 4 °C in the northern Alps (Larocque-Tobler et al., 2010), northern Italy (Heiri et al., 2007), and Jura, France (Heiri and Millet, 2005). Temperatures also increased between 2.7 and 4.0 °C in the southern Swiss Alps (Samartin et al., 2012), 2.8 °C in the southern Carpathians (Tóth et al., 2012), and 3.5–5.0 °C in Poland (Płóciennik et al., 2011). Our study site documented a 2.2 °C temperature increase at the MIS 2/MIS 1 transition, from ~11.8 ± 1.5 °C (811; sample age 14,620 cal BP) to 14.0 ± 1.4 °C (802 cm; sample age 14,550 cal BP) (Fig. 9). However, three of the four reconstructed MIS 2 temperatures must be interpreted with caution (including sample age 14,620 cal BP) due to low chironomid densities and/or because several samples had to be merged to reach minimum counts suitable for the climate reconstruction. When adjusted to 0 m asl for the end of the MIS 2 (13.7 °C - 14,660 cal BP and 12.7 °C - 14,620 cal BP), our T_{July} temperature reconstruction is ~2 °C lower than expected based on other chironomid reconstructions for 48° N in Europe (Heiri et al., 2014a). However, our coldest reconstructed T_{July} from MIS 2 overlaps with the dominance of cold stenotherm *Micropsectra radialis*-type chironomids (Fig. 9). Similarly, T_{july} are 1–2 °C lower (14.9 °C) at 14,550 cal BP during the earliest Lateglacial interstadial, although this value is only constrained by a single chironomid sample. Overall colder reconstructed temperatures in the Lateglacial interstadial may be due to a significant input of cold oxygen saturated river water when study site was likely a very shallow riverine lake possibly as shallow as 1–2 m. Such running water conditions likely enabled the persistence of more cold adapted taxa (which do not typically occur in fully lentic lake environments traditionally used for temperature reconstructions), thus giving a lower than expected temperature signal at Santovka-PB.

As a consequence of increases in both temperature and precipitation at the MIS 2/MIS 1 transition, local vegetation at Santovka-PB responded abruptly resulting in significant vegetation turnover (see macrofossil DCA scores, Fig. 10). For example, cold tolerant and rather oligotrophic aquatic species such as *Stuckenia filiformis,* which is a frequent lateglacial aquatic plant (Gałka and Sznel, 2013; Jamrichová et al., 2014; Petr et al., 2013), were replaced by more nutrient and warm-demanding species such as *Potamogeton crispus* and *Zannichellia palustris*. These warm-demanding taxa are commonly present in Holocene macrofossil records across Central Europe (e.g. Potůčková et al., 2018; Gałka et al., 2014), hence their early presence here is very striking. Their presence at Santovka-PB during the Lateglacial was probably

enabled by less stream input/impact (represented by low magnetic susceptibility values in the record) as a result of the creation of a shallow lake where gyttja (organic lake sediment with high abundance of diatom frustules) started to accumulate. The creation of a lake, which based on ERT measurements was at least 415 m in length and 130–200 m in width, could be linked with increased accumulation of travertine deposits (Fig. 4), which may have dammed the stream. Remains of *Simulium* gen. sp. (black fly) larvae (Fig. 9) and shells of the clams *Pisidium tenuilineatum* and *P. pulchellum* (Fig. 7) in the fossil record indicate that the lake had at least slow flowing water. Around the lake, species-rich and warm and nutrient-demanding wetland vegetation expanded, dominated by *Schoenoplectus tabernaemontani*, *Cicuta virosa*, *Carex caespitosa*, *Sparganium erectum*, *Lycopus europaeus*, while steppe-tundra elements *Selaginella selaginoides*, *Betula nana* and *B. humilis* were present in the surrounding landscape (Fig. 6).

Regionally, large-scale vegetation change was not evident at the MIS 2/MIS 1 transition (Fig. 8), except for the disappearance of several open-landscape taxa (e.g. *Helianthemum nummularium* t., *Dryas*, *Polemonium caeruleum*), and a slight decline in Amaranthaceae (incl. former Chenopodiaceae). Rather, a large change in the pollen record took place ~150 years later around 14,410 cal BP, when *Pinus sylvestris* pollen increased to >70% and grasses decreased to <15%. Delayed reaction of regional vegetation to rapid climate changes is seen elsewhere as a consequence of various biotic and abiotic factors, such as migrational lags (Pennington, 1986; Hoek, 2001), competition with other trees (Birks, 1986), other climatic factors such as windiness or dryness (Paus, 2010), and local edaphic conditions and abiotic landscape factors (Hoek, 2001; Ruszkiczay-Rüdiger and Kern, 2016). Short-distance migrational lag is most likely the cause of the 150-year lag at our site as the expansion of trees is a relatively slow process which may take hundreds of years (Birks, 1986). From Pannonian Basin, there is no similarly detailed paleoecological investigation suitable for a comprehensive comparison of vegetation change at the MIS 2/MIS 1 transition with our results, making our study very exceptional.

5.3. Abrupt Holocene vegetation change linked with climate fluctuations and human impact

Regionally, two Early Holocene abrupt climatic events caused changes in regional vegetation at 10,140 and ~6400 cal BP (Figs. 8 and 10). The first change around 10,140 cal BP was the result of climate amelioration at the onset of the Holocene (Fig. 8), and is characterised by a switch from open pine forests with steppe patches, to temperate broadleaf forests dominated by *Quercus*, *Corylus avellana* and *Ulmus*. Across the Danubian Lowland, this regional vegetation change was recorded within a ~3500 year interval (between 11,000 and 7500 cal BP) depending on local soil substrates, orographical and climatological conditions, and distance from refugial population from which trees could spread (Jamrichová et al., 2014, 2017; Potůčková et al., 2018; Šolcová et al., 2018). The second event occurred at 6400 cal BP when anthropogenic indicators (e.g. *Triticum*, *Polygonum aviculare*) and open-landscape taxa (e.g. Amaranthaceae, *Artemisia*) started to increase at the expense of temperate broadleaf forest taxa as a result of Late Neolithic activities. This regional event is recorded also at Santovka-village (Šolcová et al., 2018), which is ~2 km from Santovka-PB, where anthropogenic indicators and the AP/NAP ratio records a sudden decrease at around 6650 cal. BP.

Locally, abrupt changes occurred at 9,570, 8,200, 7800 and 6400 cal BP resulting in various ecological changes at Santovka-PB (Figs. 6, 7 and 10). The first abrupt change around 9570 cal BP is the result of environmental conditions changing from a shallow pool to a calcareous fen habitat, as indicated by mollusc and macrofossil results and an increase in the percentage of carbonates (Figs. 6, 7 and 10). The increase in carbonates around 9570 cal BP is interpreted as travertine precipitation enhancement, and is in congruence with results from Poland where calcareous tufa deposits peaked between 9700 and 9500 cal BP. Together, these data are indicative of a relatively humid period across the region (Starkel et al., 2012). The second local environmental change between ~8260 and 8020 cal BP (Fig. 10) is the result of travertine precipitation rates decreasing, as well as a nearly-absent macrofossil record between 8260 and 8170 cal BP. This abrupt change in the local environment is most likely linked with the cold 8.2 ka event which was recorded across Europe and in Greenland (Alley and Ágústsdóttir, 2005; LeGrande and Schmidt, 2008). The third environmental change around 7800 cal BP is likely the result of the development of a calcareous lake surrounded by rich fen taxa, as demonstrated by an abrupt decrease in percent carbonates and increase in aquatic and wetland taxa at Santovka-PB (Figs. 6 and 7). At Santovka-village (Šolcová et al., 2018), water levels also increased around 7950 cal BP indicating climate moistening. Pronounced regional climate moistening between 8000 and 7500 cal BP is also confirmed by other paleoecological data from the Western Carpathians (Dabkowski et al., 2019; Juřičková et al., 2018), and from Europe (e.g. Cvetkoska et al., 2014; Bešta et al., 2015; Kalis et al., 2003; Nádor et al., 2007; Starkel et al., 2012). The last abrupt change at 6400 cal BP is likely the result of Late Neolithic activities impacting the local environment, which generally lead to land degradation (Willis et al., 1998). Specifically, increased erosion and soil flushes from nearby fields likely led to the infilling of the lake. This is indicated by the presence of weed macrofossils (*Hyoscamus niger*, *Fumaria officinalis*) and crop pollen (*Triticum* t., *Hordeum* t.), and by increased magnetic susceptibility values (SI Fig. 1). Our results indicate that local Holocene environmental changes were closely linked to spring activity and carbonate precipitation rates, and thus indirectly to the climate, until the arrival of Late Neolithics.

5.4. Tufa or travertine deposits and their exploitation for paleoclimate reconstructions

Terrestrial limestones (or flowstones) are mainly deposited as calcite crusts by carbonate-rich waters flowing into subaerial settings, and originate either from karstic cool water springs (i.e. calcareous tufa) or from geothermal warm waters (i.e. travertine). Terrestrial limestone stable isotope ratios of carbon ($^{13}C/^{12}C$) and oxygen ($^{18}O/^{16}O$) depend mostly on the physico-chemical conditions of the water (e.g. temperature, salinity, CO_2 concentration) that promote isotopic fractionation. Fractionation, resulting from the loss due to evaporation, degassing or metabolic consumption (e.g. algae, aquatic plants) of lighter isotopes during the (bio) geochemical cycle, induces discrete changes of C and O ratios (Gandin and Capezzuoli, 2008). High values of $\delta^{13}C$ (PDB) are typical for stable isotopic data obtained from travertine deposits, range from −2‰ to +8‰, whereas $\delta^{18}O$ (PDB) values usually range from −30‰ to −4‰. For calcareous tufa, $\delta^{13}C$ and $\delta^{18}O$ values typically range from −11‰ to −5‰ and from −12‰ to −3‰, respectively (Gandin and Capezzuoli, 2008). $\delta^{13}C$ and $\delta^{18}O$ (VPDB) values at Santovka-PB ranged between −7.6‰ and +7.9‰ and −10.7‰ to −5.9‰, indicating that analysed carbonate material is travertine (Fig. 4). Together with the results from our ERT survey, our data illustrate the presence of a local tectonic fault in which hydrothermal water was able to reach the surface resulting in accumulation of travertine deposits.

Prado-Pérez et al. (2013) demonstrated that $\delta^{13}C$ values in travertine deposits are mainly controlled by both the dissolved inorganic carbon (DIC) and dissolved organic carbon (DOC) from

the surrounding parent material, which in turn is influenced by the different C sources existing in the area. When vegetation cover develops and biomass increases, the isotopic signature evolves towards more negative values due to the greater contribution of organic C, which is −27‰ vs. VPDB (Deines, 1980), to the dissolved carbon pool. Furthermore, according to Capezzuoli et al. (2014) 'travertines are linked to the availability of water, being influenced indirectly by tectonically driven ground water flow changes, which directly reflects rainfall availability and an elevated ground water'. Specifically, high amount of the rainfall could be reflected by the decrease of $\delta^{13}C$ values due to the more intense leaching of organic C from biomass and its penetration to the hydrothermal circuit. We therefore hypothesize that both higher rainfall amount and higher biomass accumulation (linked with broadleaf temperate tree expansion around 10,140 cal BP) contributed to the gradual decrease of $\delta^{13}C$ values at the beginning of the Holocene at Santovka-PB.

Prado-Pérez et al. (2013) also demonstrated that $\delta^{18}O$ values from travertine deposits reflect paleoclimatic conditions, as it corresponds to changes in their parent waters. Specifically, the isotopic signature of water is much more negative during cold and wet periods then during warm and dry periods. While our $\delta^{18}O$ record was influenced by high erosion rates during MIS 2 and the Lateglacial, and thus must be interpreted with caution, we observed an abrupt decrease in $\delta^{18}O$ values at 14,350 cal BP, interpreted as a cold oscillation. This is in congruence with T_{July}, which also illustrates a temperature decline at that time (Fig. 11). $\delta^{18}O$ values also decreased around 10,100 cal BP, likely caused by a distinct disturbance of thermohaline circulation in the North Atlantic Ocean (Bond et al., 1997; Björck et al., 2001) resulting in a short cooling event beginning around 10,300 cal BP and lasting ~200 years. Lastly, our travertine $\delta^{18}O$ values decreased around 8200 cal BP as a response to cold 8.2 ka event (Alley and Ágústsdóttir, 2005; LeGrande and Schmidt, 2008).

This study therefore highlights the importance of geothermal-related travertine precipitation and derived $\delta^{13}C$ and $\delta^{18}O$ as methods to reconstruct past abrupt climate and environmental change. Most notably, this is the first study to our knowledge to investigate isotopic signatures from travertine deposits from a precisely dated profile, together with numerous biotic and abiotic paleoecological data, allowing the cross-validation of paleoclimate reconstructions from different proxy data. Although some authors stressed that stable isotope signatures from one vertical profile from consolidated travertine deposits cannot be simply used for paleoclimatological evaluation (Kele et al., 2006), our results provide compelling evidence that $\delta^{18}O$ results from porous (i.e. fine pieces) travertine deposits reflect short-lasting climatic oscillations. However, some limitations are worth noting. Although changes in $\delta^{18}O$ values appear to correlate well with climate shifts, to disprove the influence of other drivers to $\delta^{18}O$ in travertine, further research is appropriate.

6. Conclusions

- An open steppe-tundra ecosystem dominated by Poaceae and *Pinus sylvestris* characterised the regional vegetation during the MIS 2 (17,550–14,560 cal BP), although pollen of *Quercus*, *Corylus avellana*, *Tilia* and *Alnus* was also found in small abundances, indicating our study site was in close proximity to their northern glacial refugium. A small stream surrounded by wetland grasses and/or dwarf-birch tundra was found locally.
- Open steppe-tundra was still present regionally at the beginning of MIS 1 (14,560–13,950 cal BP), however *Pinus sylvestris* began to expand. Locally, a calcareous lake with macrophytes surrounded by rich wetland vegetation and fen patches developed at Santovka-PB, although dwarf-birch tundra still surrounded the local environment. Taxa preferring higher temperatures and higher trophic states predominated in the aquatic and wetland environment.
- Two abrupt changes in regional vegetation (10,140 and 6400 cal BP) and four in the local environment (9,570, 8,200, 7800 and 6400 cal BP) were recorded during the early and middle Holocene. Local vegetation changes were related indirectly to climatic events (10,140, 9,570, ~8,200, 7800 cal BP), until 6400 cal BP when Neolithic-caused deforestation directly influenced local erosion rates and vegetation.
- Mean T_{July} increased from ~12.7 ± 1.5 °C to ~14.9 ± 1.4 °C (adjusted to modern sea level) at the MIS 2/MIS 1 transition at Santovka-PB, with biotic and abiotic proxies indicating significant humidification during this transition. Our proxies suggest wetter climatic conditions around 9570 cal BP, and abrupt humidification after 7800 cal BP, which corroborate with other paleoenvironmental records throughout Central-Eastern Europe.
- The local environment was influenced by travertine deposition around thermal springs, which occurred along a tectonic fault. $\delta^{18}O$ and $\delta^{13}C$ isotopic signatures obtained from travertine deposits demonstrate their ability to reflect short-lasting climatic

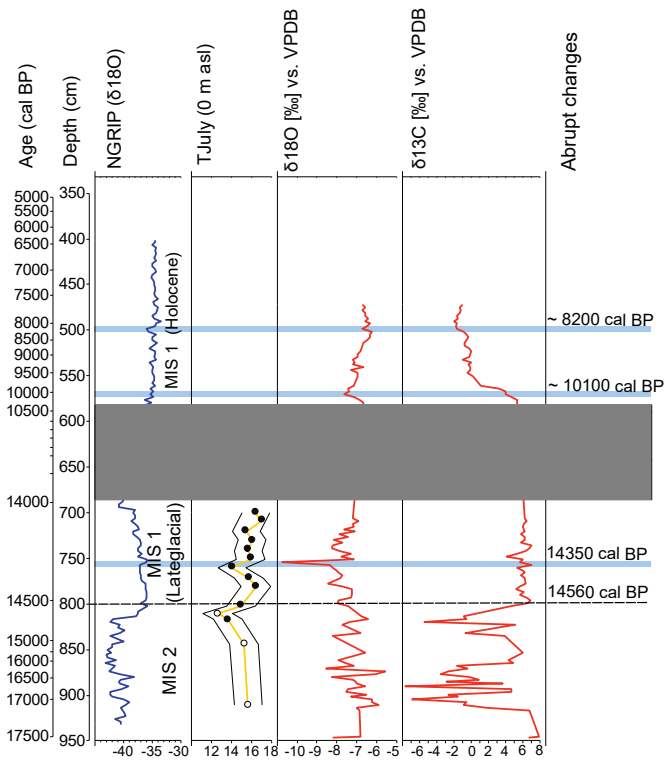

Fig. 11. $\delta^{13}C$ and $\delta^{18}O$ (Vienna Pee Dee Belemnite) from travertine deposits at Santovka-Pramene Budzgov, mean July temperature (T_{July}) and North Greenland Ice Core Project $\delta^{18}O$ data plotted on versus depth (cm) and calibrated ages (years Before Present). Displayed data were selected to demonstrate temporal changes in isotopic records together with reconstructed T_{July} and NGRIP $\delta^{18}O$ data. Abrupt changes in the fossil record are highlighted by blue horizontal lines. NGRIP $\delta^{18}O$ data (NGRIP dating group, 2006) were downloaded from ftp://ftp.ncdc.noaa.gov/pub/data/paleo/icecore/greenland/summit/ngrip/gicc05-20yr.txt. Empty circles in T_{July} curve indicate limited validity of reconstructed temperature due to a low number of individuals used in the reconstruction. Full circles display more reliable T_{July} results based on more than 35 individuals and a maximum of two adjoining depths merged together. Grey box indicates the presence of a sediment hiatus. Black dashed line indicates MIS 2/MIS 1 transition. (For interpretation of the references to colour in this figure legend, the reader is referred to the Web version of this article.)

events and major changes in the regional environment. Our results highlight the benefit of using travertine deposits, coupled with high-resolution paleoecological data, to investigate past biotic and abiotic responses to abrupt climate change.

Declaration of competing interests

The authors declare that they have no known competing financial interests or personal relationships that could have appeared to influence the work reported in this paper.

Acknowledgements

The research was funded by the Czech Science Foundation (project number, GAČR 504/17-05696S) and Charles University Grant Agency (project number, GAUK 204215). The research of A. Šolcová, P. Hájková and E. Jamrichová was also supported by the long-term research development project of the Institute of Botany of the Czech Academy of Sciences (RVO 67985939). We are very grateful to Veronika Horsáková, Ondřej Knápek, Slavo Rezník and Stanislav Němejc for their help with fieldwork. We would like to thank Vendula Vaňáčková for chironomid sample preparation, Jozef Bátora for consultation on a suitable place for the coring, Julie Dabkowski on consultation of stable isotope results and Vachel A. Carter for English correction. Access to instruments and other facilities for isotope analysis was supported by the Czech research infrastructure for systems biology C4SYS (project No LM2015055).

Appendix A. Supplementary data

Supplementary data to this article can be found online at https://doi.org/10.1016/j.quascirev.2020.106170.

References

Alley, R.B., Ágústsdóttir, A.M., 2005. The 8k event: cause and consequences of a major Holocene abrupt climate change. Quat. Sci. Rev. 24 (10–11), 1123–1149.
Ambros, C., 1977. Prírastky archeozoologického materiálu z výskumov v roku 1976. Archeologické výskumy a nálezy na Slovensku 1976, 23–29.
Bača, R., 1990. Archeologické doklady vzťahu osídlenia k minerálnym a termálnym prameňom. Balneologický spravodajca 29, 35–57.
Berger, A., Loutre, M.F., 1991. Insolation values for the climate of the last 10 million years. Quat. Sci. Rev. 10 (4), 297–317.
Berggren, G., 1969. Atlas of Seeds. Part 2. Cyperaceae, vol. 69. Swedish Museum of Natural History, Stockholm, p. 39 (plates).
Bešta, T., Novák, J., Dreslerová, D., Jankovská, V., Bernardová, A., Lisá, L., Valentová, D., 2015. Mid-holocene history of a central European lake: lake komořany, Czech Republic. Boreas 44 (3), 563–574.
Beug, H.J., 2004. Leitfaden der Pollenbestimmung für Mitteleuropa und angrenzende Gebiete. Verlag Dr. Fridrich Pfeil, München.
Birks, H.J.B., 1986. Late-Quaternary biotic changes in terrestrial and lacustrine environments, with particular reference to north-west Europe. In: Berglund, B.E. (Ed.), Handbook of Holocene Paleoecology and Paleohydrology. Wiley, Chichester, pp. 3–65.
Björck, S., Muscheler, R., Kromer, B., Andresen, C.S., Heinemeier, J., Johnsen, S.J., et al., 2001. High-resolution analyses of an early Holocene climate event may imply decreased solar forcing as an important climate trigger. Geology 29 (12), 1107–1110.
Bond, G., Showers, W., Cheseby, M., Lotti, R., Almasi, P., Priore, P., et al., 1997. A pervasive millennial-scale cycle in North Atlantic Holocene and glacial climates. Science 278 (5341), 1257–1266.
Blackmore, S., Steinmann, J.A.J., Hoen, P.P., Punt, W., 2003. Betulaceae and corylaceae. Rev. Palaeobot. Palynol. 123, 71–98.
Bojňanský, V., Fargašová, A., 2007. Atlas of Seeds and Fruits of Central and East-European Flora. The Carpathian Mountains Region. Springer, Dordrecht, p. 1046.
Bronk Ramsey, C., 2009. Bayesian analysis of radiocarbon dates. Radiocarbon 51, 337–360.
Brooks, S.J., Langdon, P.G., Heiri, O., 2007. The identification and use of Palaearctic Chironomidae larvae in paleoecology. In: QRA Technical Guide No. 10. Quaternary Research Association, London.
Budinský-Krička, V., 1941. Prehistorické nálezy z Maďaroviec v Slovenskom národnom múzeu. Časopis Muzeálnej slovenskej spoločnosti 32, 75–81.
Camill, P., Clark, J.S., 2000. Long-term perspectives on lagged ecosystem responses to climate change: permafrost in boreal peatlands and the grassland/woodland boundary. Ecosystems 3 (6), 534–544.
Capezzuoli, E., Gandin, A., Pedley, M., 2014. Decoding tufa and travertine (fresh water carbonates) in the sedimentary record: the state of the art. Sedimentology 61 (1), 1–21.
Cappers, R.T.J., Bekker, R.M., Jans, J.E.A., 2006. Digitale Zadenatlas Van Nederland. Groningen Archaeological Studies, vol. 4. Barkhuis Publishing & Groningen University Library.
Chytrý, M., Horsák, M., Danihelka, J., Ermakov, N., German, D.A., Hájek, M., Hájková, P., Kočí, M., Kubešová, S., Lustyk, P., Nekola, J.C., Pavelková Řičánková, V., Preislerová, Z., Resl, P., Valachovič, M., 2019. A modern analogue of the Pleistocene steppe-tundra ecosystem in southern Siberia. Boreas 48 (1), 36–56.
Cvetkoska, A., Levkov, Z., Reed, J.M., Wagner, B., 2014. Late Glacial to Holocene climate change and human impact in the Mediterranean: the last ca. 17 ka diatom record of Lake Prespa (Macedonia/Albania/Greece). Palaeogeogr. Palaeoclimatol. Palaeoecol. 406, 22–32.
Dabkowski, J., Frodlová, J., Hájek, M., Hájková, P., Petr, L., Fiorillo, D., Dudová, L., Horsák, M., 2019. A complete Holocene climate and environment record for the Western Carpathians (Slovakia) derived from a tufa deposit. The Holocene 28 (3), 493–504.
Dansgaard, W., Johnsen, S.J., Clausen, H.B., Dahl-Jensen, D., Gundestrup, N.S., Hammer, C.U., et al., 1993. Evidence for general instability of past climate from a 250-kyr ice-core record. Nature 364 (6434), 218–220.
De Beaulieu, J.L., Reille, M., 1992. The last climatic cycle at La Grande Pile (Vosges, France) a new pollen profile. Quat. Sci. Rev. 11 (4), 431–438.
Deines, P., 1980. The isotopic composition of reduced organic carbon. In: Fritz, P., Fontes, J.C. (Eds.), Handbook of Environmental Isotope Geochemistry. Elsevier, Amsterdam, pp. 329–406.
Eggermont, H., Heiri, O., 2012. The chironomid-temperature relationship: expression in nature and palaeoenvironmental implications. Biol. Rev. 87 (2), 430–456.
Engel, Z., Křížek, M., Kasprzak, M., Traczyk, A., Hložek, M., Krbcová, K., 2017. Geomorphological and sedimentary evidence of probable glaciation in the Jizerské hory Mountains, Central Europe. Geomorphology 280, 39–50.
Faegri, K., Kaland, P.E., Krzywinski, K., 1989. Textbook of Pollen Analysis, fourth ed. John Wiley & Sons, Chichester.
Feurdean, A., Perşoiu, A., Tanţău, I., Stevens, T., Magyari, E.K., Onac, B., et al., 2014. Climate variability and associated vegetation response throughout Central and Eastern Europe (CEE) between 60 and 8 ka. Quat. Sci. Rev. 106, 206–224.
Gałka, M., Sznel, M., 2013. Late Glacial and Early Holocene development of lakes in northeastern Poland in view of plant macrofossil analyses. Quat. Int. 292, 124–135.
Gałka, M., Tobolski, K., Zawisza, E., Goslar, T., 2014. Postglacial history of vegetation, human activity and lake-level changes at Jezioro Linówek in northeast Poland, based on multi-proxy data. Veg. Hist. Archaeobotany 23 (2), 123–152.
Gandin, A., Capezzuoli, E., 2008. Travertine versus calcareous tufa: distinctive petrologic features and stable isotopes signatures. Ital. J. Quat. Sci. 21 (1B), 125–136.
Gradziński, M., Duliński, M., Hercman, H., Stworzewicz, E., Holúbek, P., Rajnoga, P., Wróblewski, W., Kováčová, M., 2008. Facies and age of travertines from Spiš and Liptov regions (Slovakia) – preliminary results. Slov. Kras. 46 (1), 31–40.
Grimm, E.C., 2011. Tilia Software v.1, 7.16. Illinois State Museum, Springfield, IL.
Hájková, P., Jamrichová, E., Horsák, M., Hájek, M., 2013. Holocene history of a Cladium mariscus-dominated calcareous fen in Slovakia: vegetation stability and landscape development. Preslia 85 (3), 289–315.
Hájková, P., Petr, L., Horsák, M., Rohovec, J., Hájek, M., 2015. Interstadial inland dune slacks in south-west Slovakia: a multi-proxy vegetation and landscape reconstruction. Quat. Int. 357, 314–328.
Hájková, P., Pařil, P., Petr, L., Chattová, B., Grygar, T.M., Heiri, O., 2016. A first chironomid-based summer temperature reconstruction (13–5 ka BP) around 49° N in inland Europe compared with local lake development. Quat. Sci. Rev. 141, 94–111.
Heiri, O., Lotter, A.F., Lemecke, G., 2001. Loss on ignition as a method for estimating organic and carbonate content in sediments: reproducibility and comparability of results. J. Paleolimnol. 25, 101–110.
Heiri, O., Lotter, A.F., 2001. Effect of low count sums on quantitative environmental reconstructions: an example using subfossil chironomids. J. Paleolimnol. 26 (3), 343–350.
Heiri, O., Millet, L., 2005. Reconstruction of late glacial summer temperatures from chironomid assemblages in lac lautrey (Jura, France). J. Quat. Sci. 20 (1), 33–44.
Heiri, O., Filippi, M.L., Lotter, A.F., 2007. Lateglacial summer temperature in the Trentino area (Northern Italy) as reconstructed by fossil chironomid assemblages in Lago di Lavarone (1100 m asl). Acta Geol. 82, 299–308.
Heiri, O., Brooks, S.J., Birks, H.J.B., Lotter, A.F., 2011. A 274-lake calibration data-set and inference model for chironomid-based summer air temperature reconstruction in Europe. Quat. Sci. Rev. 30, 3445–3456.
Heiri, O., Brooks, S.J., Renssen, H., Bedford, A., Hazekamp, M., Ilyashuk, B., et al., 2014a. Validation of climate model-inferred regional temperature change for late-glacial Europe. Nat. Commun. 5, 4914.
Heiri, O., Koinig, K.A., Spötl, C., Barrett, S., Brauer, A., Drescher-Schneider, et al., 2014b. Palaeoclimate records 60-8 ka in the Austrian and Swiss Alps and their forelands. Quat. Sci. Rev. 106, 186–205.
Hoek, W.Z., 2001. Vegetation response to the~ 14.7 and~ 11.5 ka cal. BP climate transitions: is vegetation lagging climate? Glob. Planet. Chang. 30 (1–2), 103–115.

Horsák, M., Čejka, T., Juřičková, L., Beran, L., Horáčková, J., Hlaváč Č., J., Dvořák, L., Hájek, O., Divíšek, J., Mañas, M., Ložek, V., 2019. Check-list and distribution maps of the molluscs of the Czech and Slovak Republics. Online at: http://mollusca.sav.sk/malacology/checklist.htm. Checklist updated at 8-October-2019, maps updated at 2-October-2019.
Horsák, M., Juřičková, L., Picka, J., 2013. Měkkýši České a Slovenské Republiky. Molluscs of the Czech and Slovak Republics. Kabourek, Zlín.
Hošek, J., Lisá, L., Hambach, U., Petr, L., Vejrostová, L., Bajer, A., Grygar, T.M., Moska, P., Gottwald, Z., Horsák, M., 2017. Middle Pleniglacial pedogenesis on the northwestern edge of the Carpathian basin: A multidisciplinary investigation of the Bíňa pedo-sedimentary section, SW Slovakia. Palaeogeogr. Palaeoclimatol. Palaeoecol. 487, 321–339.
Hošek, J., Prach, J., Křížek, M., Šída, P., Moska, P., Pokorný, P., 2019. Buried late weichselian thermokarst landscape discovered in the Czech Republic, central Europe. Boreas 48 (4), 988–1005.
Jakab, J., 1977. Antropologický materiál z archeologických výskumov v roku 1976. Archeologické výskumy a nálezy na Slovensku 1976, 137–138.
Jamrichová, E., Potůčková, A., Horsák, M., Hajnalová, M., Barta, P., Tóth, P., Kuneš, P., 2014. Early occurrence of temperate oak-dominated forest in the northern part of the Little Hungarian Plain, SW Slovakia. Holocene 24 (12), 1810–1824.
Jamrichová, E., Petr, L., Jiménez-Alfaro, B., Jankovská, V., Dudová, L., Pokorný, P., Kołaczek, P., Zernitskaya, V., Černiková, M., Břízová, E., Syrovátka, V., Hájková, P., Hájek, M., 2017. Pollen-inferred millennial changes in landscape patterns at a major biogeographical interface within Europe. J. Biogeogr. 44 (10), 2386–2397.
Janek, D., 1972. Santovka. Report No. 6165/72. Archeologický ústav SAV, Nitra.
Jankovská, V., Pokorný, P., 2008. Forest vegetation of the last full-glacial period in the Western Carpathians (Slovakia and Czech Republic). Preslia 80 (3), 307–324.
Juřičková, L., Horáčková, J., Ložek, V., 2014. Direct evidence of central European forest refugia during the last glacial period based on mollusc fossils. Quat. Res. 82 (1), 222–228.
Juřičková, L., Pokorný, P., Hošek, J., Horáčková, J., Květoň, J., Zahajská, P., Jansová, A., Ložek, V., 2018. Early postglacial recolonisation, refugial dynamics and the origin of a major biodiversity hotspot. A case study from the Malá Fatra mountains, Western Carpathians, Slovakia. Holocene 28 (4), 583–594.
Kalis, A.J., Merkt, J., Wunderlich, J., 2003. Environmental changes during the Holocene climatic optimum in central Europe-human impact and natural causes. Quat. Sci. Rev. 22 (1), 33–79.
Karlén, W., Matthews, J.A., 1992. Reconstructing Holocene glacier variations from glacial lake sediments: studies from Nordvestlandet and Jostedalsbreen-Jotunheimen, southern Norway. Geogr. Ann. 74A, 327–348.
Katz, N.J., Katz, S.V., Skobeeva, E.I., 1977. Atlas of Plant Remains in Peat. Nedra, Moscow.
Kele, S., Korpás, L., Demény, A., Kovács-Pálffy, P., Bajnóczi, B., Medzihradszky, Z., 2006. Paleoenvironmental evaluation of the Tata Travertine Complex (Hungary), based on stable isotopic and petrographic studies. Acta Geol. Hungarica 49 (1), 1–31.
Kubát, K., Hrouda, L., Chrtek, J. jun, Kaplan, Z., Kirschner, J., Štěpánek, J. (Eds.), 2002. Klíč Ke Květeně České Republiky. Academia, Praha, p. 928.
Kustár, R., Molnár, D., Sümegi, P., Törőcsik, T., Sávai, S., 2016. Preliminary paleoecological reconstruction of long-term relationship between human and environment in the northern part of Danube-along Plain, Hungary. Open Geosci. 8 (1), 405–419.
Larocque-Tobler, I., Heiri, O., Wehrli, M., 2010. Late Glacial and Holocene temperature changes at Egelsee, Switzerland, reconstructed using subfossil chironomids. J. Paleolimnol. 43 (4), 649–666.
LeGrande, A.N., Schmidt, G.A., 2008. Ensemble, water isotope–enabled, coupled general circulation modeling insights into the 8.2 ka event. Paleoceanography 23 (3).
Loke, M.H., 1997. Electrical Imaging Surveys for Environmental and Engineering Studies. A Practical Guide to 2-D and 3-D Surveys, p. 61.
Lowe, J.J., Rasmussen, S.O., Björck, S., Hoek, W.Z., Steffensen, J.P., Walker, M.J., Yu, Z.C., The Intimate Group, 2008. Synchronisation of paleoenvironmental events in the North Atlantic region during the Last Termination: a revised protocol recommended by the INTIMATE group. Quat. Sci. Rev. 27 (1–2), 6–17.
Ložek, V., 1964. Quartärmollusken der Tschechoslowakei: Mit 32 fotographischen Tafeln. Nakladatelství Československé akademie věd, Praha.
Ložek, V., 2006. Last Glacial paleoenvironments of the West Carpathians in the light of fossil malacofauna. Antropozoikum 26, 73–84.
Magyari, E., Jakab, G., Rudner, E., Sümegi, P., 1999. Palynological and plant macrofossil data on Late Pleistocene short-term climatic oscillations in NE-Hungary. Acta Palaeobot. 2, 491–502.
Magyari, E., Sümegi, P., Braun, M., Jakab, G., Molnár, M., 2001. Retarded wetland succession: anthropogenic and climatic signals in a Holocene peat bog profile from north-east Hungary. J. Ecol. 89 (6), 1019–1032.
Magyari, E.K., Jakab, G., Sümegi, P., Szöőr, G., 2008. Holocene vegetation dynamics in the Bereg Plain, NE Hungary–the Báb-tava pollen and plant macrofossil record. Acta Geogr. Debrecina 42, 1–16.
Magyari, E.K., Chapman, J.C., Passmore, D.G., Allen, J.R.M., Huntley, J.P., Huntley, B., 2010. Holocene persistence of wooded steppe in the Great Hungarian Plain. J. Biogeogr. 37 (5), 915–935.
Nádor, A., Thamó-Bozsó, E., Magyari, Á., Babinszki, E., 2007. Fluvial responses to tectonics and climate change during the Late Weichselian in the eastern part of the Pannonian Basin (Hungary). Sediment. Geol. 202 (1–2), 174–192.
Nagy, A., 1998. Geologická Mapa Podunajskej Nížiny – Východná Časť 1: 50 000. In: Halouzka, R., Konečný, V., Dublan, L., Havrila, M., Lexa, J., Pristaš, J. (Eds.). MŽP SR – GSSR, Bratislava.
Nekola, J.C., Chiba, S., Coles, B.F., Drost, C.A., von Proschwitz, T., Horsák, M., 2018. A phylogenetic overview of the genus Vertigo O. F. Müller, 1773 (Gastropoda: pulmonata: pupillidae: vertigininae). Malacologia 62, 21–161.
NGRIP dating group, 2006. Greenland ice core chronology 2005 (GICC05). In: IGBP PAGES/World Data Center for Paleoclimatology. Data Contribution Series # 2006-118. NOAA/NCDC Paleoclimatology Program, Boulder CO, USA.
Paus, A., 2010. Vegetation and environment of the Rødalen alpine area, Central Norway, with emphasis on the early Holocene. Veg. Hist. Archaeobotany 19 (1), 29–51.
Pavúk, J., 1977. Nálezisko lengyelskej a badenskej kultúry v Santovke a Domadiciach. Archeologické výskumy a nálezy na Slovensku 1976, 221–222.
Pavúk, J., 1987. Sídlisko lengyelskej kultúry v Santovke a Domadiciach. Archeologické výskumy a nálezy na Slovensku 1986, 84–85.
Pavúk, J., 1994. Santovka – eine bedeutende Fundstelle der Lengyel-Kultur in der Slowakei. Archaol. Korresp. 24, 167–177.
Pavúk, J., 1997. Kockovité a zoomorfné dózičky lengyelskej kultúry zo Santovky. Sb. Pr. Filoz. Fak. Brnenské Univ. M2, 65–77.
Pennington, W., 1986. Lags in adjustment of vegetation to climate caused by the pace of soil development. Evidence from Britain. Vegetatio 67 (2), 105–118.
Petr, L., Žáčková, P., Grygar, T.M., Píšková, A., Křížek, M., Treml, V., 2013. Šúr, a former late-glacial and Holocene lake at the westernmost margin of the Carpathians. Preslia 85 (3), 239–263.
Płóciennik, M., Self, A., Birks, H.J.B., Brooks, S.J., 2011. Chironomidae (Insecta: Diptera) succession in zabieniec bog and its paleo-lake (central Poland) through the late weichselian and holocene. Paleogeogr., Paleoclimatology, Paleoecology 307 (1–4), 150–167.
Potůčková, A., Hájková, P., Žáčková, P., Petr, L., Grygar, T.M., Weiser, M., 2018. Spatiotemporal heterogeneity of the paleoecological record in a large temperate paleolake, Šúr, southwest Slovakia: comparison of pollen, macrofossil and geochemical data. Paleogeogr., Paleoclimatology, Paleoecology 489, 52–63.
Prado-Pérez, A.J., Huertas, A.D., Crespo, M.T., Sánchez, A.M., Perez Del Villar, L., 2013. Late Pleistocene and Holocene mid-latitude paleoclimatic and paleoenvironmental reconstruction: an approach based on the isotopic record from a travertine formation in the Guadix-Baza basin, Spain. Geol. Mag. 150 (4), 602–625.
Punt, W., Clarke, G.C.S. (Eds.), 1984. The Northwest European Pollen Flora, IV. Elsevier, Amsterdam.
Quinlan, R., Smol, J.P., 2001. Setting minimum head capsule abundance and taxa deletion criteria in chironomid-based inference models. J. Paleolimnol. 26 (3), 327–342.
Randsalu-Wendrup, L., Conley, D.J., Carstensen, J., Snowball, I., Jessen, C., Fritz, S.C., 2012. Ecological regime shifts in Lake Källksjön, Sweden, in response to abrupt climate change around the 8.2 ka cooling event. Ecosystems 15 (8), 1336–1350.
Rasmussen, S.O., Andersen, K.K., Svensson, A.M., Steffensen, J.P., Vinther, B.M., Clausen, H.B., Bigler, M., et al., 2006. A new Greenland ice core chronology for the last glacial termination. J. Geophys. Res. 111 (D06102).
Rasmussen, S.O., Bigler, M., Blockley, S.P., Blunier, T., Buchardt, S.L., Clausen, H.B., et al., 2014. A stratigraphic framework for abrupt climatic changes during the Last Glacial period based on three synchronized Greenland ice-core records: refining and extending the INTIMATE event stratigraphy. Quat. Sci. Rev. 106, 14–28.
Reille, M., 1992. Pollen et spores D'Europe et D'Afrique du Nort. Laboratoire de botanique historique et palynologie, Marseille.
Reimer, P.J., Bard, E., Bayliss, A., Beck, J.W., Blackwell, P.G., Bronk Ramsey, C., et al., 2013. IntCal13 and Marine 13 radiocarbon age calibration curves 0–50,000 years cal BP. Radiocarbon 55, 1869–1887.
Ruszkiczay-Rüdiger, Z., Kern, Z., 2016. Permafrost or seasonal frost? A review of paleoclimate proxies of the last glacial cycle in the East Central European lowlands. Quat. Int. 415, 241–252.
Samartin, S., Heiri, O., Vescovi, E., Brooks, S.J., Tinner, W., 2012. Lateglacial and early Holocene summer temperatures in the southern Swiss Alps reconstructed using fossil chironomids. J. Quat. Sci. 27 (3), 279–289.
Samartin, S., Heiri, O., Joos, F., Renssen, H., Franke, J., Brönnimann, S., Tinner, W., 2017. Warm Mediterranean mid-Holocene summers inferred from fossil midge assemblages. Nat. Geosci. 10 (3), 207.
Shakesby, R.A., Smith, J.G., Matthews, J.A., Winkler, S., Dresser, P.Q., Bakke, J., Dahl, S.O., Lie, Ø., Nesje, A., 2007. Reconstruction of Holocene glacier history from distal sources: glaciofluvial streambank mires and a glaciolacustrine sediment core near Sota Sæter, Breheimen, southern Norway. Holocene 17 (6), 729–745.
Šolcová, A., Petr, L., Hájková, P., Petřík, J., Tóth, P., Rohovec, J., Bátora, J., Horsák, M., 2018. Early and middle Holocene ecosystem changes at the Western Carpathian/Pannonian border driven by climate and Neolithic impact. Boreas 47 (3), 897–909.
Starkel, L., Michczyńska, D., Krazpiec, M., Margielewski, W., Nalepka, D., Pazdur, A., 2012. Progress in the Holocene chrono-climatostratigraphy of polish territory. Geochronometria 40, 1–21.
Sümegi, P., Molnár, M., Jakab, G., Persaits, G., Majkut, P., Páll, D.G., Gulyás, S., Jull, A.J.T., Törcsik, T., 2011. Radiocarbon-dated paleoenvironmental changes on a lake and peat sediment sequence from the central Great Hungarian Plain (Central Europe) during the last 25,000 years. Radiocarbon 53 (1), 85–97.
Sümegi, P., Gulyás, S., Csökmei, B., Molnár, D., Hambach, U., Stevens, T., Markovic, S.B., Almond, P.C., 2012. Climatic fluctuations inferred for the Middle

and Late Pleniglacial (MIS 2) based on high-resolution (~ ca. 20 y) preliminary environmental magnetic investigation of the loess section of the Madaras brickyard (Hungary). Central European Geology 55 (3), 329–345.
Sümegi, P., Magyari, E., Dániel, P., Molnár, M., Törőcsik, T., 2013. Responses of terrestrial ecosystems to Dansgaard–Oeshger cycles and Heinrich-events: a 28,000-year record of environmental changes from SE Hungary. Quat. Int. 293, 34–50.
Sümegi, P., Náfrádi, K., 2015. A radiocarbon-dated cave sequence and the Pleistocene/Holocene transition in Hungary. Open Geosci. 7 (1).
Ter Braak, C.J.F., Šmilauer, P., 2012. Canoco Reference Manual and User's Guide: Software for Ordination, Version 5.0. Microcomputer Power, Ithaca, USA, p. 496.
Tóth, M., Magyari, E.K., Brooks, S.J., Braun, M., Buczkó, K., Bálint, M., Heiri, O., 2012. A chironomid-based reconstruction of late glacial summer temperatures in the southern Carpathians (Romania). Quat. Res. 77 (1), 122–131.
Tzedakis, P.C., Emerson, B.C., Hewitt, G.M., 2013. Cryptic or mystic? Glacial tree refugia in northern Europe. Trends Ecol. Evol. 28 (12), 696–704.
Van Geel, B., Bohncke, S.J.P., Dee, H., 1980. A palaeoecological study of an upper late glacial and Holocene sequence from "de Borchert", The Netherlands. Rev. Palaeobot. Palynol. 31, 367–448.
Van Raden, U.J., Colombaroli, D., Gilli, A., Schwander, J., Bernasconi, S.M., van Leeuwen, J., et al., 2013. High-resolution late-glacial chronology for the Gerzensee lake record (Switzerland): δ18O correlation between a Gerzensee-stack and NGRIP. Palaeogeogr. Palaeoclimatol. Palaeoecol. 391, 13–24.
Velichkevich, F.Y., Zastawniak, E., 2006. Atlas of the Pleistocene Vascular Plant Macrofossils of Central and Eastern Europe. Part 1–Pteridophytes and Monocotyledons. W. Szafer Instytute of Botany, Polish Academy of Sciences, Kraków.
Velichkevich, F.Y., Zastawniak, E., 2008. Atlas of the Pleistocene Vascular Plant Macrofossils of Central and Eastern Europe. Part 2–Herbaceous Dicotyledons. W. Szafer Instytute of Botany, Polish Academy of Sciences, Kraków.
Chironomidae of the holarctic region: keys and diagnoses. Part I - larvae. In: Wiederholm, T. (Ed.), Entomol. Scand. Suppl. 19, 1–457.
Willis, K.J., Sümegi, P., Braun, M., Tóth, A., 1995. The Late Quaternary environmental history of Bátorliget, N.E. Hungary. Palaeogeogr. Palaeoclimatol. Palaeoecol. 118, 25–47.
Willis, K.J., Sümegi, P., Braun, M., Bennett, K.D., Tóth, A., 1998. Prehistoric land degradation in Hungary: who, how and why? Antiquity 72, 101–113.
Willis, K.J., Rudner, E., Sümegi, P., 2000. The full-glacial forests of central and southeastern Europe. Quat. Res. 53 (2), 203–213.
Willis, K.J., Van Andel, T.H., 2004. Trees or no trees? The environments of central and eastern Europe during the Last Glaciation. Quat. Sci. Rev. 23 (23–24), 2369–2387.
Willis, K.J., Birks, H.J.B., 2006. What is natural? The need for a long-term perspective in biodiversity conservation. Science 314 (5803), 1261–1265.